

NAVAL POSTGRADUATE SCHOOL

Monterey, California



THESIS

**ELECTRONIC COUNTER-COUNTER MEASURES
POTENTIAL OF A NONCOHERENT FH/MFSK
COMMUNICATIONS SYSTEM UNDER CONDITIONS OF
WORST CASE HOSTILE ELECTRONIC COUNTER
MEASURES AND FADING CHANNELS**

by
George T. Katsoulis
March, 1997

Thesis Advisor:

R. Clark Robertson

Thesis
K145366

Approved for public release; distribution is unlimited.

DUDLEY KNOX LIBRARY
NAVAL POSTGRADUATE SCHOOL
MONTEREY CA 93943-5101

DUDLEY KNOX LIBRARY
NAVAL POSTGRADUATE SCHOOL
MONTEREY CA 93943-5101

REPORT DOCUMENTATION PAGE

Form Approved
OMB No. 0704-0188

Public reporting burden for this collection of information is estimated to average 1 hour per response, including the time for reviewing instruction, searching existing data sources, gathering and maintaining the data needed, and completing and reviewing the collection of information. Send comments regarding this burden estimate or any other aspect of this collection of information, including suggestions for reducing this burden, to Washington headquarters Services, Directorate for Information Operations and Reports, 1215 Jefferson Davis Highway, Suite 1204, Arlington, VA 22202-4302, and to the Office of Management and Budget, Paperwork Reduction Project (0704-0188) Washington DC 20503.

1. AGENCY USE ONLY (Leave blank)

2. REPORT DATE
March 1997

3. REPORT TYPE AND DATES COVERED
Master's Thesis, Final

4. TITLE AND SUBTITLE ELECTRONIC COUNTER-COUNTER MEASURES POTENTIAL OF A NONCOHERENT FH/MFSK COMMUNICATIONS SYSTEM UNDER CONDITIONS OF WORST CASE HOSTILE ELECTRONIC COUNTER MEASURES AND FADING CHANNELS

5. FUNDING NUMBERS

6. AUTHOR(S)
Katsoulis George

7. PERFORMING ORGANIZATION NAME(S) AND ADDRESS(ES)
Naval Postgraduate School
Monterey, CA 93943-5000

8. PERFORMING
ORGANIZATION REPORT
NUMBER

9. SPONSORING / MONITORING AGENCY NAME(S) AND ADDRESS(ES)

10. SPONSORING /
MONITORING
AGENCY REPORT NUMBER

11. SUPPLEMENTARY NOTES

The views expressed in this thesis are those of the author and do not reflect the official policy or position of the Department of Defense or the U.S. Government.

12a. DISTRIBUTION / AVAILABILITY STATEMENT
Approved for public release; distribution unlimited.

12b. DISTRIBUTION CODE

13. ABSTRACT (maximum 200 words)

This thesis investigates the performance degradation resulting from multitone interference of orthogonal, noncoherent, frequency-hopped, M-ary frequency-shift keyed receivers (FH/MFSK) where the effect of thermal and other wideband noise is not neglected. The multiple, equal power jamming tones are assumed to correspond to some or all of the possible FH M-ary orthogonal signaling tones. Furthermore, the channel is modeled as a Ricean fading channel, a possibility precluded when thermal noise is neglected. Both the signaling tones and the multiple interference tones are assumed to be affected by channel fading. Both band and independent band multitone interference are considered. Performance is evaluated by obtaining a union bound on the probability of bit error, and receiver performance is compared with exact results for band multitone interference of a noncoherent FH/MFSK receiver under comparable circumstances. Except for the case of Rayleigh fading of the signal, the union bound is very tight for those cases that can be compared with exact results. The advantages of the union bound approach are twofold. First, the union bound approach yields a solution that is far less computationally intensive than that obtained with the exact approach. Second, the union bound approach allows numerical results to be obtained for interference conditions that are not amenable to exact analysis, such as independent multitone interference of FH/MFSK.

14. SUBJECT TERMS

Frequency-Hopping, Ricean Fading Channel, Union Bound Approach, Band Multitone Interference, Independent Multitone Interference

15. NUMBER OF
PAGES 96

16. PRICE CODE

SECURITY CLASSIFICATION OF
REPORT
Unclassified

18. SECURITY CLASSIFICATION OF
THIS PAGE
Unclassified

19. SECURITY CLASSIFICATION
OF ABSTRACT
Unclassified

20. LIMITATION
OF ABSTRACT
UL

Approved for public release; distribution is unlimited

**ELECTRONIC COUNTER-COUNTER MEASURES POTENTIAL OF A
NONCOHERENT FH/MFSK COMMUNICATIONS SYSTEM UNDER
CONDITIONS OF WORST CASE HOSTILE ELECTRONIC COUNTER
MEASURES AND FADING CHANNELS**

George T. Katsoulis
Lieutenant JG, Hellenic Navy
B.S.E.E, Hellenic Naval Academy, 1989

Submitted in partial fulfillment of the
requirements for the degree of

MASTER OF SCIENCE IN ELECTRICAL ENGINEERING

NPS Archive
1997.03
Katsoulis, G

~~THOSE~~
~~A 1/5~~
C.2

ABSTRACT

This thesis investigates the performance degradation resulting from multitone interference on orthogonal, noncoherent, frequency-hopped, M-ary frequency-shift keyed receivers (FH/MFSK) where the effect of thermal and other wideband noise is not neglected. The multiple, equal power jamming tones are assumed to correspond to some or all of the possible FH M-ary orthogonal signaling tones. Furthermore, the channel is modeled as a Ricean fading channel, a possibility precluded when thermal noise is neglected. Both the signaling tones and the multiple interference tones are assumed to be affected by channel fading. Both band and independent band multitone interference are considered. Performance is evaluated by obtaining a union bound on the probability of bit error, and receiver performance is compared with exact results for band multitone interference of a noncoherent FH/MFSK receiver under comparable circumstances. Except for the case of Rayleigh fading of the signal, the union bound is very tight for those cases that can be compared with exact results. The advantages of the union bound approach are twofold. First, the union bound approach yields a solution that is far less computationally intensive than that obtained with the exact approach. Second, the union bound approach allows numerical results to be obtained for interference conditions that are not amenable to exact analysis, such as independent multitone interference of FH/MFSK.

TABLE OF CONTENTS

I. INTRODUCTION	1
A. SCOPE OF THESIS	1
B. IMPORTANCE OF A SPREAD SPECTRUM COMMUNICATION SYSTEM.....	2
II. IMPORTANCE OF UNION BOUND APPROACH	3
III. BACKGROUND	5
IV. FH/MFSK SYSTEM, CHANNEL MODEL, AND SYMBOLOGY USED	9
V. FH/MFSK RECEIVER PERFORMANCE WITH INDEPENDENT MULTITONE INTERFERENCE	13
A. $\Pr(R_1 < R_2 l)$	19
B. $\Pr(R_1 < R_2 l, S_{j_1})$	22
C. $\Pr(R_1 < R_2 l, S_{j_2})$	28
D. $\Pr(R_1 < R_2 l, S_{j_1}, S_{j_2})$	34
VI. FH/MFSK RECEIVER PERFORMANCE WITH BAND MULTITONE INTERFERENCE	37
VII. NUMERICAL RESULTS	41
A. BAND MULTITONE INTERFERENCE	42
B. INDEPENDENT MULTITONE INTERFERENCE	45
VIII. CONCLUSION	49
REFERENCES	77
APPENDIX. MATHEMATICAL IDENTITIES AND RELATIONS	79
INITIAL DISTRIBUTION LIST	87

THE UNIVERSITY OF CHICAGO

THE UNIVERSITY OF CHICAGO

THE UNIVERSITY OF CHICAGO

THE UNIVERSITY OF CHICAGO

THE UNIVERSITY OF CHICAGO

THE UNIVERSITY OF CHICAGO

THE UNIVERSITY OF CHICAGO

THE UNIVERSITY OF CHICAGO

THE UNIVERSITY OF CHICAGO

THE UNIVERSITY OF CHICAGO

THE UNIVERSITY OF CHICAGO

THE UNIVERSITY OF CHICAGO

THE UNIVERSITY OF CHICAGO

THE UNIVERSITY OF CHICAGO

I. INTRODUCTION

A. SCOPE OF THESIS

The goal of this thesis is to determine the electronic counter-counter measures (ECCM) potential of a non-coherent frequency-hopped M-ary frequency-shift keying (FH/MFSK) communication system under conditions of worst case hostile electronic counter measures (ECM) and fading channels. The performance of the FH/MFSK receiver will be investigated for frequency-nonselective, slowly fading Ricean channels and hostile multitone interference.

The receiver considered uses a quadratic detector in each M-ary branch of the receiver for signal detection. Both band and independent multitone interference are considered and both jammer and signal are assumed to be affected by the fading channel, where it is also assumed that the channel fading need not necessarily affect the signaling tones and the interference tones in the same way. The cases of Rayleigh, Ricean, and no fading are all considered.

Performance is evaluated by obtaining a union bound on the probability of bit error. The results are compared with the exact results, examined in [1], to determine the accuracy of the union bound approach. Then the union bound is used to obtain probability of bit error for situations where the exact approach is either very difficult or even impossible to obtain.

B. IMPORTANCE OF A SPREAD SPECTRUM COMMUNICATION SYSTEM

The benefit from investigating the performance of a spread spectrum communication system lies in the extent to which spread spectrum communications are currently used. Their application to any military communication system aids in achieving

secure, low probability of intercept, and/or low probability of detection information exchange between friendly units as well as reducing the ability of hostile elements to jam friendly communications. Other applications of spread spectrum are:

1) The use of either frequency-hopping or direct sequence spread spectrum in multiple access communications (as in cellular phones where vehicles communicate with a central station) in which a number of independent users are required to share a common channel without an external synchronization mechanism.

2) The application of spread spectrum techniques in wireless local area networks (LANs). Wireless LANs are very important for the establishment of a network for mobile forces that circulates among the cooperating units various kinds of information, such as text messages, video, or audio. Wireless LANs are also very popular in commercial communications and are used for wireless communication of laptop computers with a control station.

In any case, the potential of frequency-hopping spread spectrum to reject interference of either unintended or intended transmissions with the communicating signal is of crucial importance. The problem considered in this thesis is the evaluation of the performance of a frequency-hopped system in order to determine the system's capabilities and limitations.

In chapters 2, 3, and 4, the union bound approach to performance analysis, a brief description of frequency-hopping, and the notation used in the thesis are discussed. In chapters 5 and 6, receiver performance with independent and band multitone jamming, respectively, are analyzed. In chapter 7 numerical results for both independent and band multitone jamming are presented.

II. IMPORTANCE OF UNION BOUND APPROACH

The union bound approach simplifies the mathematical development by deriving an expression for the upper bound on the probability of symbol error that is always much simpler than the exact form. There are usually two approaches used to evaluate the probability of symbol error of a communications system.

In the first approach, known as the indirect approach, the probability of symbol error is obtained using the relation

$$P_s = 1 - \bar{P}_s \quad (1)$$

where \bar{P}_s is the probability of not making a symbol error. Noting by X_1, X_2, \dots, X_M the random variables representing the output of each branch of the receiver for a signal with M symbols, we have:

$$P_s = 1 - \bar{P}_s = 1 - \Pr(X_1 > X_2 \cap X_1 > X_3 \cap \dots \cap X_1 > X_M | 1). \quad (2)$$

The calculation of this probability is difficult, especially in the case where we deal not only with gaussian noise but also with jammer tones affecting the signal. This will become particularly obvious later on when we analyze receiver performance with independent multitone interference. In that case, the joint probability distribution functions required to solve the problem using the exact solution approach make it impossible to obtain a closed form expression for the probability of symbol error for a system using more than two symbols.

However, if we use the union bound, or direct approach, the solution works as follows, providing an upper bound to the probability of error calculation:

$$P_s = \Pr(X_1 < X_2 \cup X_1 < X_3 \cup \dots \cup X_1 < X_M | I) \leq \Pr(X_1 < X_2 | I) + \Pr(X_1 < X_3 | I) + \dots + \Pr(X_1 < X_M | I) \quad (3)$$

We see that in place of joint probability distribution functions (pdfs) we now have the sum of individual pdfs. In fact, the individual pdfs can be grouped in groups of identical pdfs occurring with a certain multiplicity, so that the solution is a linear combination of a few pdfs.

Summarizing, the union bound approach provides a simple, fast method to investigate communication and jammer signal scenarios that are very difficult, if not impossible, to explore with the exact result approach as described in [1]. By using the union bound, we can increase our knowledge of communication systems performance for a larger variety of jamming conditions. However, since this evaluation is a bound, its accuracy, or tightness, needs to be tested so that we can comment on its effectiveness and limitations as a tool. In fact, in the following pages it will be shown that in some cases the union bound approach is so accurate that it provides virtually identical results with the exact solution, while in some other cases the results obtained display an anomalous behavior.

III. BACKGROUND

The main idea of frequency-hopping spread spectrum communications is to provide protection against a hostile jammer by increasing the bandwidth that the information signal occupies much more than the minimum required. By increasing the frequency range over which a system effectively operates, we force the jammer to spread its power over a wider frequency band and thus be less effective from a "per-frequency" signal corruption capability point of view.

The main idea of frequency-hopping spread spectrum is based on the multiplication of the signal prior to transmission by an intermediate frequency, generated by a frequency synthesizer, of the form

$$f_i = f_1 + (i - 1) \cdot \Delta f_{fh} \text{ where } i=1,2,\dots,N \quad (4)$$

where N is the maximum number of possible frequency hop bins, Δf_{fh} is the separation between the carrier frequencies of adjacent bins, and 'i' changes pseudo-randomly every T_c seconds. By so doing, the entire spectrum of the signal transmitted, is shifted from its carrier frequency f_c to the new carrier frequencies:

$$f_{c_i} = f_c + f_1 + (i - 1) \cdot \Delta f_{fh} . \quad (5)$$

The result is that a new data modulated carrier that is shifted from one frequency to the next is created. From (5) we see that there are N different frequency hop bins, each of bandwidth Δf_{fh} . The value of i (and thus f_{c_i}) is changed periodically according to some predetermined, but apparently random to a third party observer, noiselike spreading code called either the pseudo-random or the pseudo-noise (PN) sequence.

Generally, frequency-hopping is used with noncoherent modulation formats such as noncoherent MFSK. Such a signal is described by:

$$s(t) = \sqrt{2}A_c \cos[2\pi(f_s + (m-1) \cdot \Delta_f)t + \theta_i] \quad (6)$$

where $m=1,2,\dots,M$, θ_i is the i^{th} symbol phase, and Δ_f is the frequency separation between each of the M signaling tones. Multiplying this signal by a signal at the intermediate frequency $f_i = f_1 + (i-1) \cdot \Delta f_{\text{fh}}$, we get:

$$\begin{aligned} s'(t) &= 2\sqrt{2}A_c \cos\{2\pi[f_s + (m-1)\Delta_f]t + \theta_i\} \cos(2\pi f_i t) = \\ &= \sqrt{2}A_c \cos\{2\pi[f_i + f_s + (m-1)\Delta_f]t + \theta_i\} + \sqrt{2}A_c \cos\{2\pi[f_i - f_s - (m-1)\Delta_f]t + \theta_i\} \end{aligned} \quad (7)$$

The carrier frequencies of the first part are

$$f_i + f_s + (m-1)\Delta_f = f_1 + (i-1)\Delta f_{\text{fh}} + f_s + (m-1)\Delta_f \quad (8)$$

and is smallest for $i=1$ and $m=1$; i.e., $f_s + f_1$. The carrier frequencies of the second part are

$$f_i - f_s - (m-1)\Delta_f = f_1 + (i-1)\Delta f_{\text{fh}} - f_s - (m-1)\Delta_f \quad (9)$$

and is largest for $i=N$ and $m=1$; i.e.,

$$f_1 + (N-1)\Delta f_{\text{fh}} - f_s. \quad (10)$$

If the smallest frequency of the first part is greater than the largest frequency of the second part, then

$$2f_s > 2f_1 + 2B + (N-1)\Delta f_{fh} \Rightarrow f_s > f_1 + B + (N-1)\Delta f_{fh} / 2 \quad (11)$$

where B is the required guardband above and below the high and the low frequency signaling tones respectively. In this case, the signal $s'(t)$ can be high-pass filtered to remove the frequency difference contribution, and the frequency-hopped signal becomes:

$$\sqrt{2}A_c \cos\{2\pi[f_i + f_s + (m-1)\Delta f_r]t + \theta_i\} \quad (12)$$

One obvious advantage is that a hostile jammer needs to know the pseudo-noise sequence of the communicator's transmitter in order to jam the specific hop bin where the transmitter operates at each time instant. To overcome a follower jammer, the signal must hop to a new carrier frequency before the jammer is able to complete its tracking process.

Another advantage is due to the fact that the power spectral density of the frequency-hopped signal is identical to the that of the conventional signal in a specific hop bin. However, since the signal hops from bin to bin, and assuming that the probability that any bin is occupied is equal to $(1/N)$, the average power spectral density is:

$$\text{PSD} = \frac{1}{N} \cdot \sum_{i=1}^N S_{\text{FSK}}(f | f_c = f_{c_i}) \quad (13)$$

Hence, the signal power spectral density is lowered by a factor of N on average.

Before proceeding we need to distinguish between the two main tone jammer methods used against communication systems. The first is band multitone interference and the second is independent multitone interference. In each case, we assume that the

multiple jamming tones are all of equal power. In band multitone interference, the multiple equal power jamming tones are distributed randomly across the entire frequency hop bandwidth, but the number of jamming tones placed within each jammed frequency hopped band is specific. In independent multitone interference, the multiple equal power jamming tones are distributed in a completely random fashion, meaning that the number of jammer tones within a frequency hop bin can vary from zero to a maximum equal to the total number of signal tones corresponding to each symbol the communicator can use. We also assume that each jamming tone corresponds exactly to one of the possible $M \times N$ signaling tones. From the communicator's viewpoint, this is the worst case.

Before proceeding to the analysis of the receiver performance with multitone jamming, the notation used in the remainder of the thesis is discussed in the next chapter.

IV. FH/MFSK SYSTEM, CHANNEL MODEL, AND SYMBOLOGY USED

The FH/MFSK communication system examined is assumed to have N non-overlapping FH bins. The bandwidth of each one is B Hz, where B is the bandwidth of the non-hopped MFSK signal. So the total frequency-hopped bandwidth is augmented to be greater than or equal to $B \cdot N$. We also express by M the modulation order where

$$M = 2^k \quad (14)$$

and k is the number of bits per M -ary symbol. Since the number of signal tones within a hop bin is M and the total number of bins is N , the result is a total of $M \cdot N$ possible signal tone locations.

The symbol duration T_s is related to the hop duration T_c by:

$$T_c = K \cdot T_s \quad (15)$$

where $K=1,2,3,\dots$. The symbol and hop rates are the reciprocal of the corresponding durations, so

$$R_s = \frac{1}{T_s} \quad (16)$$

$$\text{and } R_c = \frac{1}{T_c}, \quad (17)$$

respectively. Symbol rate is related to hop rate by

$$R_s = K \cdot R_c \quad (18)$$

Using the frequency hopped signal (12), we note that the M symbols are assumed to be equally likely, both f_i and f_s are taken to be integer multiples of the symbol rate R_s , and the frequency difference between signal tones Δ_f is taken to be an integer multiple of the symbol rate. Hence,

$$\Delta_f = p \cdot R_s \text{ (p integer)}. \quad (19)$$

To incorporate the idea of fading channels, we model the amplitude A_c as a Ricean random variable. This includes Rayleigh fading as a specific case.

The transmitter and receiver are assumed to function in perfect synchronization, and the receiver after dehopping the signal uses a bank of M quadrature detectors where the integrator time constants are normalized to the symbol duration for notational convenience (Figure 1).

The existing noise interference is expressed as AWGN with a flat average power spectral density defined as $\frac{N_0}{2}$. The total power of the jammer is expressed as P_{J_T} , and the jammer delivers q equal power interfering tones such that the power of a single interfering tone is equal to

$$P_j = \frac{P_{J_T}}{q}. \quad (20)$$

The subscripts used in the description of the Ricean random variables are 'c' for the signal parameters and 'j' for the jammer. Thus, the pdf of A_c is

$$f_{A_c}(a_c) = \frac{a_c}{\sigma_c^2} \cdot \exp\left(-\frac{a_c^2 + \alpha_c^2}{2\sigma_c^2}\right) \cdot \text{Io}\left(\frac{a_c^2 \cdot \alpha_c^2}{\sigma_c^2}\right) \cdot u(a_c) \quad (21)$$

where $u(\bullet)$ is the unit step function, $I_0(\bullet)$ is the modified Bessel function of the first kind and order zero, α^2_c is the power of the direct signal component, and $2\sigma^2_c$ is the power of the diffuse signal component of the respective tone. The total average power of either a Ricean faded jammer or signal tone is equal to the mean squared value of the amplitude a_c or a_j , respectively, and is

$$\bar{P}_i = \alpha^2_i + 2\sigma^2_i \quad (i = c, j). \quad (22)$$

The average power is assumed to remain constant from hop to hop. It is convenient to define the signal-to-noise power ratios of the direct signal components as

$$\rho_i = \frac{\alpha^2_i}{\sigma^2_n} \quad (i = c, j) \quad (23)$$

and the diffuse signal components as

$$\xi_i = \frac{2\sigma^2_i}{\sigma^2_n} \quad (i = c, j) \quad (24)$$

where σ^2_n is the noise power.

For orthogonal signaling, the average probability of bit error is related to the average probability of symbol error by [2]

$$P_b = \frac{M/2}{M-1} \cdot P_s, \quad (25)$$

and the average energy per bit is related to the average energy per symbol by

$$E_s = \log_2(M) \cdot E_b = k \cdot E_b. \quad (26)$$

V. FH/MFSK RECEIVER PERFORMANCE WITH INDEPENDENT MULTITONE INTERFERENCE

With independent multitone interference, the multiple, equal power jamming tones are distributed randomly across the entire frequency-hopped bandwidth. Two possible cases exist concerning the signal and jammer tones within a specific frequency-hop bin. In the first case there is no interference at all in the bin (the jammer tones are elsewhere), and the probability of error is the same as for a conventional MFSK signal in the presence of AWGN only. In the second case there is jammer interference in the bin. Since a bin is composed of M different signal locations and a potential jammer may place one or more of its tones to the aforementioned signal locations, this case is further divided into two subcases. In the first subcase the signal and jammer tones are on different branches, while in the second subcase one jammer tone coincides with a signal tone. This gives a total of three individual cases that are treated below.

Case 1:

In the following, we express by R_1, R_2, \dots, R_M the random variables representing the outputs of branches 1, 2, ..., M , respectively, of an MFSK receiver. Without loss of generality, we assume that the symbol '1' is transmitted. In order not to have an error, the output of branch one must be greater than the outputs of all other branches. The opposite situation expresses the error condition. As in equation (2), the probability of symbol error provided by the union bound is

$$\begin{aligned}
 P_s &= \Pr(R_1 < R_2 \cup R_1 < R_3 \cup \dots \cup R_1 < R_M | 1) \\
 &\leq \Pr(R_1 < R_2 | 1) + \Pr(R_1 < R_3 | 1) + \dots + \Pr(R_1 < R_M | 1) \\
 &\leq (M - 1) \cdot \Pr(R_1 < R_2 | 1)
 \end{aligned} \tag{27}$$

and the last equation is true since the individual probabilities are equal.

Case 2a:

Suppose that we have L jammer tones in the hop bin where the signal is. By S_j we express the existence of a jammer tone, and the subscript after j corresponds to the specific branch where the jammer tone is present. For example S_{j_1} means that a jammer tone is present in branch one. To simplify the discussion for this case, suppose that we have two jammer tones ($L=2$). Now

$$\begin{aligned} \Pr(\text{error}|l, S_{j_2}, S_{j_3}) &\leq \Pr(R_1 < R_2|l, S_{j_2}) + \Pr(R_1 < R_3|l, S_{j_3}) + \Pr(R_1 < R_4|l) + \dots + \Pr(R_1 < R_M|l) \\ \text{Since } \Pr(R_1 < R_4|l) &= \Pr(R_1 < R_5|l) = \dots = \Pr(R_1 < R_M|l) = \\ &= \Pr(\text{error with no interference in signal branch}) \end{aligned} \quad (28)$$

$$\text{and } \Pr(R_1 < R_2|l, S_{j_2}) = \Pr(R_1 < R_3|l, S_{j_3}). \quad (29)$$

then (28) reduces to

$$\Pr(\text{error}|l, S_{j_2}, S_{j_3}) \leq 2 \Pr(R_1 < R_2|l, S_{j_2}) + (M - 3) \cdot \Pr(R_1 < R_4|l) \quad (30)$$

Generalizing for L jamming tones per hop bin, $1 \leq L \leq M-1$, we get

$$\Pr(\text{error}|l, \sum_{i=1}^L S_{j_{i+1}}) \leq L \cdot \Pr(R_1 < R_2|l, S_{j_2}) + (M - L - 1) \cdot \Pr(R_1 < R_M|l) \quad (31)$$

Case 2b:

As with case 2a, we begin by considering two jammer tones. In this case

$$\begin{aligned} \Pr(\text{error}|l, S_{j_1}, S_{j_2}) &\leq \Pr(R_1 < R_2|l, S_{j_1}, S_{j_2}) + \Pr(R_1 < R_3|l, S_{j_1}) + \Pr(R_1 < R_4|l, S_{j_1}) + \dots \\ &+ \Pr(R_1 < R_M|l, S_{j_1}) \end{aligned} \quad (32)$$

As before, this can be simplified to

$$\Pr(\text{error}|l, S_{j_1}, S_{j_2}) \leq \Pr(R_1 < R_2|l, S_{j_1}, S_{j_2}) + (M - 2) \cdot \Pr(R_1 < R_2|l, S_{j_1}). \quad (33)$$

Generalizing, for L jamming tones per hop bin, $1 \leq L \leq M-1$, we get

$$\Pr(\text{error}|l, S_{j_1}, \sum_{i=2}^L S_{j_{i+1}}) = (L - 1) \cdot \Pr(R_1 < R_2|l, S_{j_1}, S_{j_2}) + (M - L) \cdot \Pr(R_1 < R_M|l, S_{j_1})$$

where it is understood that the summation is zero for $L = 1$.

(34)

Now the probability of symbol error with at least one jamming tone per hop bin ($L \geq 1$) is given by:

$$\Pr(\text{error}) = \Pr(\text{error}|l, \sum_{i=1}^L S_{j_{i+1}}) \cdot \Pr(1, \sum_{i=1}^L S_{j_{i+1}}) + \Pr(\text{error}|l, S_{j_1}, \sum_{i=2}^L S_{j_{i+1}}) \cdot \Pr(1, S_{j_1}, \sum_{i=2}^L S_{j_{i+1}}) \quad (35)$$

Since we have L jammer tones and M signaling tones per jammed frequency-hop bin,

$$\Pr(1, S_{j_1}, \sum_{i=2}^L S_{j_{i+1}}) = \frac{L}{M} \quad (36)$$

$$\text{and } \Pr(1, \sum_{i=1}^L S_{j_{i+1}}) = 1 - \frac{L}{M}. \quad (37)$$

So the probability of symbol error for L jamming tones per hop bin, $L \geq 1$, is given by

$$\begin{aligned}
P_s(L) \leq & \frac{L}{M} \cdot \left[(L-1) \cdot \Pr(R_1 < R_2 | l, S_{j_1}, S_{j_2}) + (M-L) \cdot \Pr(R_1 < R_M | l, S_{j_1}) \right] + \\
& + \left(1 - \frac{L}{M} \right) \cdot \left[L \cdot \Pr(R_1 < R_2 | l, S_{j_2}) + (M-L-1) \cdot \Pr(R_1 < R_M | l) \right]
\end{aligned} \tag{38}$$

We now look for the probability of having L jamming tones per hop bin. This leads to the expression for the total probability of bit error. For independent multitone interference, and since we assume q jamming tones randomly interfere with a total of $N \cdot M$ possible signal tones, $1 \leq q \leq N \cdot M$, the probability that a frequency-hop bin contains one interfering tone is

$$\frac{q}{N \cdot M} . \tag{39}$$

The probability that a frequency hop bin contains a second interfering tone is

$$\frac{q-1}{N \cdot M - 1} . \tag{40}$$

The probability that a frequency hop does not contain an interfering tone is

$$1 - \frac{q}{N \cdot M} \tag{41}$$

The probability that a frequency hop bin does not contain a second interference tone is

$$1 - \frac{q-1}{N \cdot M - 1} . \tag{42}$$

From (39) - (42), we derive the probability that a frequency hop bin contains **no** interference tones as

$$\left(1 - \frac{q}{N \cdot M}\right) \cdot \left(1 - \frac{q}{N \cdot M - 1}\right) \cdot \dots \cdot \left(1 - \frac{q}{N \cdot M - (M - 1)}\right) = \prod_{i=0}^{M-1} \left(1 - \frac{q}{N \cdot M - i}\right) \quad (43)$$

Similarly, the probability that there is one jamming tone in a frequency hop bin is

$$\begin{aligned} & \frac{q}{M \cdot N} \cdot \left[\left(1 - \frac{q-1}{N \cdot M - 1}\right) \cdot \left(1 - \frac{q-1}{N \cdot M - 2}\right) \cdot \dots \cdot \left(1 - \frac{q-1}{N \cdot M - (M-1)}\right) \right] = \\ & = \frac{q}{M \cdot N} \prod_{i=1}^{M-1} \left(1 - \frac{q-1}{N \cdot M - i}\right) \end{aligned} \quad (44)$$

In the same manner, we define the probability that there are two jamming tones in a frequency hop bin as

$$\begin{aligned} & \frac{q}{M \cdot N} \cdot \frac{q-1}{N \cdot M - 1} \left[\left(1 - \frac{q-2}{N \cdot M - 1}\right) \cdot \left(1 - \frac{q-2}{N \cdot M - 2}\right) \cdot \dots \cdot \left(1 - \frac{q-2}{N \cdot M - (M-1)}\right) \right] = \\ & = \prod_{i=0}^1 \left(\frac{q-i}{M \cdot N - i} \right) \cdot \prod_{i=1}^{M-1} \left(1 - \frac{q-2}{M \cdot N - i}\right). \end{aligned} \quad (45)$$

Combining (43), (44), and (45), we get the probability that L jamming tones are in a hop bin, where $1 \leq L < M-1$, as

$$\begin{aligned}
\Pr(L \text{ jamming tones per hop bin}) &= \left[\frac{q}{M \cdot N} \cdot \frac{q-1}{M \cdot N - 1} \cdots \frac{q-(L-1)}{M \cdot N - (L-1)} \right] \cdot \\
&\cdot \left[1 - \frac{q-(L-1)-1}{M \cdot N - (L-1)-1} \right] \cdots \left[1 - \frac{q-(L-1)-1}{M \cdot N - (M-1)} \right] \\
&= \left[\prod_{i=0}^{L-1} \frac{q-i}{M \cdot N - i} \right] \cdot \left[\prod_{i=L}^{M-1} \left(1 - \frac{q-(L-1)-1}{M \cdot N - i} \right) \right]
\end{aligned} \tag{46}$$

The situation where $L=M$ must be treated separately. Looking at the two individual products multiplied together in (46), we see that the first product has L terms, corresponding to the probability that L out of the M signals of the bin are jammed, while the second product has the remaining $M-L$ signals of the bin which are not jammed. Since when $L=M$ all the signals are jammed, for that case we need only the first product term. So the probability of having $L=M$ jamming tones in a hop bin is

$$\Pr(L = M) = \prod_{i=0}^{L-1} \frac{q-i}{M \cdot N - i} \tag{47}$$

Now, the total probability of symbol error for $0 \leq L \leq M$ is given by

$$\Pr(\text{error}) = \Pr(L = 0) \cdot P_s(1) + \Pr(L = 1) \cdot P_s(1|L = 1) + \dots + \Pr(L = M) \cdot P_s(1|L = M) \tag{48}$$

The maximum number of jamming tones we can have in a bin is M if $M < q$ and q if $q < M$. This can be represented as $\min(q, M)$. By combining equations (46), (47), and (48), the probability of symbol error is given by the relation

$$\begin{aligned}
P_s \leq & \left\{ \prod_{i=0}^{M-1} \left(1 - \frac{q}{N \cdot M - i} \right) \right\} \cdot (M-1) \Pr(R_1 < R_2 | l) + \\
& + \left\{ \sum_{L=1}^{\min(M-1, q)} \left[\prod_{i=0}^{L-1} \frac{q-i}{M \cdot N - i} \right] \cdot \left[\prod_{i=L}^{M-1} \left(1 - \frac{q - (L-1) - 1}{M \cdot N - i} \right) \right] \right\} \cdot P_s(L) + \\
& + \left\{ \prod_{i=0}^{L-1} \frac{q-i}{M \cdot N - i} \right\} \cdot P_s(M)
\end{aligned} \tag{49}$$

The probability $P_s(M)$ is obtained by letting $L=M$ in (38). This yields

$P_s(M) = (M-1) \cdot \Pr(R_1 < R_2 | l, S_{j_1}, S_{j_2})$. Based on the above probabilistic description, it

is apparent that we need to obtain the following probabilities for the MFSK receiver:

$\Pr(R_1 < R_2 | l)$, $\Pr(R_1 < R_2 | l, S_{j_1})$, $\Pr(R_1 < R_2 | l, S_{j_2})$,

and $\Pr(R_1 < R_2 | l, S_{j_1}, S_{j_2})$.

A. $\Pr(R_1 < R_2 | l)$

For noncoherent, orthogonal BFSK, $\Pr(R_1 < R_2 | l)$ is equivalent to the probability of bit error:

$$P_b(a_c) = \frac{1}{2} \cdot e^{-\frac{a_c^2}{2\sigma_n^2}} \tag{50}$$

$$\text{where } \sigma_n^2 = \frac{N_o}{T_b}. \tag{51}$$

For noncoherent, orthogonal MFSK, the only thing that changes is that T_b is replaced by T_s :

$$\sigma_n^2 = \frac{N_0}{T_s}. \quad (52)$$

To account for the existence of a Ricean fading channel we multiply equation (50) with (21), the Ricean pdf, and then integrate over all possible values of a_c . This yields

$$\begin{aligned} P_b &= \int_0^\infty P_b(a_c) \cdot f_{A_c}(a_c) da_c = \int_0^\infty \frac{1}{2} \cdot \exp\left(-\frac{a_c^2}{2\sigma_n^2}\right) \cdot \frac{a_c}{\sigma_c^2} \cdot \exp\left[-\frac{a_c^2 + \alpha_c^2}{2\sigma_c^2}\right] \cdot I_0\left(\frac{\alpha_c \cdot a_c}{\sigma_c^2}\right) \cdot u(a_c) \\ &= \frac{1}{2\sigma_c^2} \cdot \exp\left[\frac{-\alpha_c^2}{2\sigma_c^2}\right] \cdot \int_0^\infty a_c \cdot \exp\left[-\frac{a_c^2}{2}\left(\frac{1}{\sigma_n^2} + \frac{1}{\sigma_c^2}\right)\right] \cdot I_0\left(\frac{\alpha_c a_c}{\sigma_c^2}\right) da_c \end{aligned} \quad (53)$$

Let $x = a_c^2 \Rightarrow dx = 2a_c da_c$, and (53) becomes:

$$P_b = \frac{1}{4\sigma_c^2} \cdot \exp\left[\frac{\alpha_c^2}{2\sigma_c^2}\right] \cdot \int_0^\infty a_c \cdot \exp\left[-\frac{x}{2}\left(\frac{1}{\sigma_n^2} + \frac{1}{\sigma_c^2}\right)\right] \cdot I_0\left(\frac{\alpha_c \sqrt{x}}{\sigma_c^2}\right) da_c. \quad (54)$$

We then use the identity [3]:

$$\int_0^\infty x^{\frac{m+n}{2}} \cdot e^{-ax} \cdot J_n(2\beta\sqrt{x}) dx = \frac{m! \beta^n \exp\left[-\frac{\beta^2}{a}\right]}{a^{m+n+1}} \mathfrak{I}_m^n\left(\frac{\beta^2}{a}\right) \quad (55)$$

where $\mathfrak{I}_m^n(\bullet)$ is the Laguerre polynomial and is defined [3]:

$$\mathfrak{I}_m^n \left(\frac{\beta^2}{a} \right) = \sum_{p=0}^m \frac{(-1)^p}{p!} \cdot \binom{m+n}{m-p} \cdot \left(\frac{\beta^2}{a} \right)^p. \quad (56)$$

In our case $m=n=0$ and the whole polynomial evaluates to unity. In place of "a" we have

$\frac{1}{2} \left(\frac{1}{\sigma_n^2} + \frac{1}{\sigma_c^2} \right)$ while in place of "β" we have $\frac{j\alpha_c}{\sigma_c^2}$. So,

$$\begin{aligned} P_b &= \frac{1}{4\sigma_c^2} \cdot \exp \left[-\frac{\alpha_c^2}{2\sigma_c^2} \right] \cdot \int_0^\infty \exp(-\alpha x) \cdot J_0(2\beta\sqrt{x}) dx = \\ &= \frac{1}{4\sigma_c^2} \cdot \exp \left[-\frac{\alpha_c^2}{2\sigma_c^2} \right] \cdot \left(\frac{2\sigma_c^2\sigma_n^2}{\sigma_c^2 + \sigma_n^2} \right) \cdot \exp \left[\left(\frac{\alpha_c^2}{4\sigma_c^4} \right) \left(\frac{2\sigma_c^2\sigma_n^2}{\sigma_c^2 + \sigma_n^2} \right) \right] = \\ &= \frac{1}{2 + 2 \cdot \frac{\sigma_c^2}{\sigma_n^2}} \cdot \exp \left[-\frac{\alpha_c^2}{2\sigma_c^2} \left(1 - \frac{\sigma_n^2}{\sigma_c^2 + \sigma_n^2} \right) \right] = \frac{1}{2 + 2 \cdot \frac{\sigma_c^2}{\sigma_n^2}} \cdot \exp \left[-\frac{\alpha_c^2}{2\sigma_c^2 + \sigma_n^2} \right]. \quad (57) \end{aligned}$$

Using (23) and (24), we have the definitions:

$$\begin{aligned} p_c &= \text{direct signal-to-noise-ratio} = \frac{\alpha_c^2}{\sigma_n^2} \\ \xi_c &= \text{diffuse signal-to-noise-ratio} = \frac{2\sigma_c^2}{\sigma_n^2} \end{aligned}$$

Applying these definitions to (57), we get

$$\Pr(R_1 < R_2 | 1) = \frac{1}{2 + \xi_c} \cdot \exp \left[-\frac{p_c}{2 + \xi_c} \right]. \quad (58)$$

B. $\Pr(R_1 < R_2 | I, S_{j_1})$

This probability of error is the same as that derived in section 4.A except that a jammer tone is on the signal branch. Since signal and jammer tone exist on same branch, we can consider that they constitute a new kind of (altered) signal existing on the branch. So the probabilistic analysis yields the same result with the only difference being that the "old" signal power a_c^2 is replaced by

$$a_c^2 + a_j^2 + 2a_c a_j \cos\theta_j. \quad (59)$$

In other words, the power of the signal and jammer tones add together but not necessarily in phase. We then integrate with respect to θ_j after multiplying by its pdf to eliminate the dependence on θ . The phase angle θ_j is assumed to be uniformly distributed in $[0, 2\pi]$.

Without jamming, the mean values of the random variables representing the outputs of the in-phase and quadrature components of the first branch are given by:

$$X_{i_1} = \sqrt{2}a_c \cos(\theta) \quad (60)$$

$$X_{q_1} = \sqrt{2}a_c \sin(\theta) \quad (61)$$

and in this case the output of the first branch is given by:

$$X_{i_1}^2 + X_{q_1}^2 = 2a_c^2 (\cos^2(\theta) + \sin^2(\theta)) = 2a_c^2 \quad (62)$$

This results in the probability of error:

$$\Pr(R_1 < R_2|l) = \frac{1}{2} \exp\left(-\frac{a_c^2 T_s}{2N_o}\right). \quad (63)$$

With jamming we have for the in-phase, quadrature components, and their squared sum as the final branch output the following relations, respectively,

$$X_{i_l} = \sqrt{2}a_c \cos(\theta) + \sqrt{2}a_j \cos(\theta'_j) \quad (64)$$

$$X_{q_l} = \sqrt{2}a_c \sin(\theta) + \sqrt{2}a_j \sin(\theta'_j) \quad (65)$$

$$\text{and } X_{i_l}^2 + X_{q_l}^2 = 2\left[a_c^2 + a_j^2 + 2a_c a_j \cos(\theta - \theta'_j)\right] \quad (66)$$

We define $\theta_j = \theta - \theta'_j$ as the phase of the jammer with respect to the received signal to get the final form of equation (59). Considering the equations above, we can understand why we substitute the previous signal power a_c^2 in $\Pr(R_1 < R_2|l, S_{j_1})$ by the composite power $a_c^2 + a_j^2 + 2a_c a_j \cos(\theta_j)$. Substituting (59) into (63), multiplying by

$f_{\theta_j}(\theta_j) = \frac{1}{2\pi}$, and integrating over θ_j , we get

$$\Pr(R_1 < R_2|l, S_{j_1}) = \frac{1}{4\pi} \cdot \int_0^{2\pi} \exp\left(-\frac{a_c^2 + a_j^2 + 2a_c a_j \cos(\theta_j)}{2N_o}\right) d\theta_j. \quad (67)$$

We then use the identity

$$I_0(z) = \frac{1}{2\pi} \cdot \int_0^{2\pi} \exp[\pm z \cdot \cos(\phi - \theta)] d\phi \quad (68)$$

to obtain

$$\begin{aligned} \Pr(R_1 < R_2 | l, S_{j_1}) &= \frac{1}{2} \cdot \exp\left[-\frac{a_c^2}{2\sigma_n^2} \left(1 + \frac{a_j^2}{a_c^2}\right)\right] \cdot I_0\left(\frac{a_c^2}{\sigma_n^2} \cdot \frac{a_j}{a_c}\right) \\ &= \frac{1}{2} \cdot \exp\left[-\frac{1}{2\sigma_n^2} (a_c^2 + a_j^2)\right] \cdot I_0\left(\frac{a_c \cdot a_j}{\sigma_n^2}\right). \end{aligned} \quad (69)$$

However, this probability of error is conditional on both a_j and a_c . To eliminate the dependence on a_c , we multiply by its pdf (Ricean) and then integrate for all possible values of a_c . After multiplying (69) by (21) and integrating, we get:

$$\begin{aligned} \Pr(R_1 < R_2 | l, S_{j_1}) &= \frac{1}{2} \cdot \exp\left[-\frac{1}{2\sigma_n^2} (a_j^2)\right] \cdot \int_0^\infty a_c \cdot \frac{1}{\sigma_c^2} \cdot \exp\left[-\frac{1}{2\sigma_n^2} (a_c^2)\right] \cdot \exp\left[-\frac{a_c^2 + \alpha_c^2}{2\sigma_c^2}\right] \cdot I_0\left(\frac{a_c \cdot a_j}{\sigma_n^2}\right) \cdot I_0\left(\frac{a_c \cdot \alpha_c}{\sigma_c^2}\right) da_c \\ &= \frac{1}{2\sigma_c^2} \cdot \exp\left[-\frac{1}{2\sigma_n^2} (a_j^2)\right] \cdot \exp\left[-\frac{\alpha_c^2}{2\sigma_c^2}\right] \cdot \int_0^\infty a_c \cdot \exp\left[-\frac{\sigma_c^2 + \sigma_n^2}{2\sigma_c^2 \sigma_n^2} (a_c^2)\right] \cdot I_0\left(\frac{a_c \cdot a_j}{\sigma_n^2}\right) \cdot I_0\left(\frac{a_c \cdot \alpha_c}{\sigma_c^2}\right) da_c \end{aligned} \quad (70)$$

We now have the identity[3]:

$$\int_0^{\infty} x \cdot \exp[-ax^2] \cdot I_n(\beta x) \cdot J_n(\gamma x) dx = \frac{1}{2a} \cdot \exp\left[\frac{\beta^2 - \gamma^2}{4a}\right] \cdot J_n\left(\frac{\beta\gamma}{2a}\right). \quad (71)$$

The correspondence of the terms in (70) with the ones in the identity are:

$$a = \frac{\sigma_c^2 + \sigma_n^2}{2\sigma_c^2 \sigma_n^2}, \quad \beta = \frac{a_j}{\sigma_n^2}, \quad \gamma = \frac{j \cdot \alpha_c}{\sigma_c^2}.$$

So the probability of error, after eliminating the dependence on a_c , is

$$\Pr(R_1 < R_2 | l, S_{j_l}) = \frac{\sigma_n^2}{2(\sigma_c^2 + \sigma_n^2)} \cdot \exp\left(-\frac{1}{2} \cdot \frac{a_j^2 + \alpha_c^2}{\sigma_c^2 + \sigma_n^2}\right) \cdot I_0\left(\frac{\alpha_c}{\sigma_c^2 + \sigma_n^2} \cdot a_j\right). \quad (72)$$

To eliminate the dependence on a_j , we multiply by its pdf (Ricean) and then integrate for all possible values of a_j . The Ricean pdf for a_j is given by:

$$f_{A_j}(a_j) = \frac{a_j}{\sigma_j^2} \cdot \exp\left[-\frac{a_j^2 + \alpha_j^2}{2\sigma_j^2}\right] \cdot I_0\left(\frac{\alpha_j \cdot a_j}{\sigma_j^2}\right) \cdot u(a_j). \quad (73)$$

Multiplying equation (72) by (73), we get:

$$\frac{\sigma_n^2}{2(\sigma_c^2 + \sigma_n^2)} \cdot \exp\left(-\frac{1}{2} \cdot \frac{a_j^2 + \alpha_c^2}{\sigma_c^2 + \sigma_n^2}\right) \cdot \left(\frac{a_j}{\sigma_j^2} \cdot \exp\left(-\frac{a_j^2 + \alpha_j^2}{2\sigma_j^2}\right)\right) \cdot I_0\left(\frac{\alpha_c}{\sigma_c^2 + \sigma_n^2} \cdot a_j\right) \cdot I_0\left(\frac{\alpha_j \cdot a_j}{\sigma_j^2}\right)$$

$$\begin{aligned}
&= \frac{\sigma_n^2}{2(\sigma_c^2 + \sigma_n^2)} \cdot \frac{a_j}{\sigma_j^2} \cdot \exp\left(-\frac{1}{2} \cdot \frac{\sigma_j^2 a_j^2 + \sigma_j^2 \alpha_c^2 + \sigma_c^2 a_j^2 + a_j^2 \sigma_n^2 + \alpha_j^2 \sigma_c^2 + \alpha_j^2 \sigma_n^2}{(\sigma_c^2 + \sigma_n^2) \sigma_j^2}\right) \cdot \\
&\quad I_0\left(\frac{\alpha_c}{\sigma_c^2 + \sigma_n^2} \cdot a_j\right) \cdot I_0\left(\frac{\alpha_j \cdot a_j}{\sigma_j^2}\right) \\
&= \frac{1}{2} \cdot \frac{\sigma_n^2}{\sigma_j^2 (\sigma_c^2 + \sigma_n^2)} \cdot \frac{a_j}{\sigma_j^2} \exp\left(-\frac{1}{2} \cdot \frac{\sigma_j^2 + (\sigma_c^2 + \sigma_n^2)}{(\sigma_c^2 + \sigma_n^2) \sigma_j^2}\right) \cdot \\
&\quad \cdot \exp\left(-\frac{1}{2} \cdot \frac{\sigma_j^2 \alpha_c^2 + (\alpha_j^2 \sigma_c^2 + \alpha_j^2 \sigma_n^2)}{(\sigma_c^2 + \sigma_n^2) \sigma_j^2}\right) \cdot I_0\left(\frac{\alpha_c}{\sigma_c^2 + \sigma_n^2} \cdot a_j\right) \cdot I_0\left(\frac{\alpha_j \cdot a_j}{\sigma_j^2}\right)
\end{aligned} \tag{74}$$

To integrate (74) with respect to a_j we again use identity (71). The correspondence of the terms in (74) with the equivalent ones of the identity are:

$$a = \frac{1}{2} \cdot \frac{\sigma_j^2 + (\sigma_c^2 + \sigma_n^2)}{(\sigma_c^2 + \sigma_n^2) \sigma_j^2}, \quad \beta = \frac{\alpha_c}{\sigma_c^2 + \sigma_n^2}, \quad \gamma = j \cdot \frac{\alpha_j}{\sigma_j^2}$$

For the argument of the Bessel function, we have:

$$\frac{\beta \gamma}{2a} = \frac{\frac{\alpha_c}{\sigma_c^2 + \sigma_n^2} \cdot \left(j \cdot \frac{\alpha_j}{\sigma_j^2}\right)}{2 \left[\frac{1}{2} \cdot \frac{\sigma_j^2 + (\sigma_c^2 + \sigma_n^2)}{(\sigma_c^2 + \sigma_n^2) \sigma_j^2} \right]} = j \cdot \frac{\alpha_c \alpha_j}{\sigma_j^2 + \sigma_c^2 + \sigma_n^2}$$

$$\text{So the final Bessel function has the form: } I_0\left(\frac{\alpha_c \alpha_j}{\sigma_j^2 + \sigma_c^2 + \sigma_n^2}\right) \tag{75}$$

$$\text{Now, } \frac{1}{2a} = \frac{1}{2 \left[\frac{1}{2} \cdot \frac{\sigma_j^2 + \left(\frac{\alpha_c \alpha_j}{\sigma_j^2 + \sigma_c^2 + \sigma_n^2} \right)}{(\sigma_c^2 + \sigma_n^2) \sigma_j^2} \right]} = \frac{(\sigma_c^2 + \sigma_n^2) \sigma_j^2}{\sigma_j^2 + \sigma_c^2 + \sigma_n^2}$$

So the terms appearing in front of the integral of (74) reduce to:

$$\frac{1}{\sigma_j^2 + \sigma_c^2 + \sigma_n^2} \cdot (\sigma_c^2 + \sigma_n^2) \cdot \sigma_j^2 \cdot \left[\frac{1}{2} \cdot \frac{\sigma_n^2}{\sigma_j^2 (\sigma_c^2 + \sigma_n^2)} \right] = \frac{\sigma_n^2}{2(\sigma_j^2 + \sigma_c^2 + \sigma_n^2)} \quad (76)$$

Finally, the argument of the $\exp(\bullet)$ function that the integral of (74) yields is:

$$\frac{\beta^2 - \gamma^2}{4a} = \frac{\left(\frac{\alpha_c}{\sigma_c^2 + \sigma_n^2} \right)^2 - \left(j \cdot \frac{\alpha_j}{\sigma_j^2} \right)}{4 \cdot \left[\frac{1}{2} \cdot \frac{\sigma_j^2 + (\sigma_c^2 + \sigma_n^2)}{(\sigma_c^2 + \sigma_n^2) \sigma_j^2} \right]}$$

and combining this with the leading exponential functions we get the final exponential function to be of the form:

$$\frac{\left(\frac{\alpha_c}{\sigma_c^2 + \sigma_n^2} \right)^2 - \left(j \cdot \frac{\alpha_j}{\sigma_j^2} \right)}{4 \cdot \left[\frac{1}{2} \cdot \frac{\sigma_j^2 + (\sigma_c^2 + \sigma_n^2)}{(\sigma_c^2 + \sigma_n^2) \sigma_j^2} \right]} - \frac{1}{2} \cdot \frac{\sigma_j^2 \alpha_c^2 + (\alpha_j^2 \sigma_c^2 + \alpha_j^2 \sigma_n^2)}{(\sigma_c^2 + \sigma_n^2) \sigma_j^2} = -\frac{1}{2} \cdot \frac{(\alpha_c^2 + \alpha_j^2)}{\sigma_j^2 + \sigma_c^2 + \sigma_n^2} \quad (77)$$

Combining (75), (76), and (77) as required by (71) we get:

$$\Pr(R_1 < R_2 | l, S_{j_1}) = \frac{\sigma_n^2}{2(\sigma_j^2 + \sigma_c^2 + \sigma_n^2)} \cdot \exp\left(-\frac{1}{2} \cdot \frac{\alpha_c^2 + \alpha_j^2}{\sigma_j^2 + \sigma_c^2 + \sigma_n^2}\right) \cdot I_0\left(\frac{\alpha_c \alpha_j}{\sigma_j^2 + \sigma_c^2 + \sigma_n^2}\right) \quad (78)$$

Substituting

$$\rho_c = \frac{\alpha_c^2}{\sigma_n^2}, \quad \rho_j = \frac{\alpha_j^2}{\sigma_n^2}, \quad \xi_c = \frac{2\sigma_c^2}{\sigma_n^2}, \quad \xi_j = \frac{2\sigma_j^2}{\sigma_n^2}$$

in (78), we get

$$\Pr(R_1 < R_2 | l, S_{j_1}) = \frac{1}{\xi_j + \xi_c + 2} \cdot \exp\left(-\frac{\rho_c + \rho_j}{\xi_j + \xi_c + 2}\right) \cdot I_0\left(\frac{2\sqrt{\rho_c \rho_j}}{\xi_j + \xi_c + 2}\right) \quad (79)$$

C. $\Pr(R_1 < R_2 | l, S_{j_2})$

We begin by designating V_1 and V_2 to be the random variables representing the outputs of branch 1 (where the signal resides) and branch 2 (where the jammer tone resides), respectively. Their pdfs are given by

$$f_{V_1}(v_1 | l, a_c) = \frac{1}{2\sigma_n^2} \cdot \exp\left(-\frac{v_1 + 2a_c^2}{2\sigma_n^2}\right) \cdot I_0\left[\frac{a_c \cdot \sqrt{2v_1}}{\sigma_n^2}\right] \quad (80)$$

$$f_{V_2}(v_2 | l, a_j) = \frac{1}{2\sigma_n^2} \cdot \exp\left(-\frac{v_2 + 2a_j^2}{2\sigma_n^2}\right) \cdot I_0\left[\frac{a_j \cdot \sqrt{2v_2}}{\sigma_n^2}\right] \quad (81)$$

Multiplying (80) by (21) and integrating, we get

$$f_{V_1}(v_1|l) = \frac{1}{2\sigma_n^2 \cdot \sigma_c^2} \cdot \exp\left(-\frac{\alpha_c^2}{2\sigma_c^2}\right) \cdot \exp\left(-\frac{v_1}{2\sigma_n^2}\right) \cdot \int_0^\infty a_c \cdot \exp\left(-a_c^2 \cdot \frac{\sigma_n^2 + 2\sigma_c^2}{2\sigma_n^2 \sigma_c^2}\right) \cdot I_0\left(\frac{a_c \sqrt{2v_1}}{\sigma_n^2}\right) \cdot I_0\left(\frac{a_c \alpha_c}{\sigma_c^2}\right) da_c \quad (82)$$

We then use the identity given in (71) where

$$a = \frac{\sigma_n^2 + 2 \cdot \sigma_c^2}{2\sigma_n^2 \sigma_c^2}, \quad \beta = \frac{\sqrt{2v_1}}{\sigma_n^2}, \quad \gamma = j \frac{\alpha_c}{\sigma_c^2} \quad (83)$$

Now we have

$$\frac{\beta \cdot \gamma}{2a} = \frac{\frac{\sqrt{2v_1} \alpha_c}{\sigma_n^2 \sigma_c^2}}{\frac{\sigma_n^2 + 2\sigma_c^2}{\sigma_n^2 \sigma_c^2}} = \frac{\sqrt{2v_1} \alpha_c}{\sigma_n^2 + 2\sigma_c^2} \quad (84)$$

$$\frac{\beta^2 - \gamma^2}{4a} = \frac{\frac{2v_1}{\sigma_n^4} + \frac{\alpha_c^2}{\sigma_c^4}}{\frac{2(\sigma_n^2 + 2\sigma_c^2)}{\sigma_n^2 \sigma_c^2}} = \frac{2v_1 \sigma_c^4 + \sigma_n^4 \alpha_c^2}{2(\sigma_n^2 + 2\sigma_c^2) \sigma_n^2 \sigma_c^2} \quad (85)$$

Hence, using (83), (84), (85) in (71), we can evaluate (82) to obtain

$$f_{V_1}(v_1|l) = \frac{1}{2(\sigma_n^2 + 2\sigma_c^2)} \cdot \exp\left(-\frac{1}{2} \cdot \frac{v_1 + 2\alpha_c^2}{\sigma_n^2 + 2\sigma_c^2}\right) \cdot I_0\left(\frac{\sqrt{2v_1} \cdot \alpha_c}{\sigma_n^2 + 2\sigma_c^2}\right) \quad (86)$$

Similarly,

$$f_{V_2}(v_2|S_{j_2}) = \frac{1}{2(\sigma_n^2 + 2\sigma_j^2)} \cdot \exp\left(-\frac{1}{2} \cdot \frac{v_2 + 2\alpha_j^2}{\sigma_n^2 + 2\sigma_j^2}\right) \cdot I_0\left(\frac{\sqrt{2v_2} \cdot \alpha_j}{\sigma_n^2 + 2\sigma_j^2}\right) \quad (87)$$

Using the random variable transformation $R_1^2 = V_1$, we get

$$f_{R_1}(R_1|l) = \frac{r_1}{(\sigma_n^2 + 2\sigma_c^2)} \cdot \exp\left(-\frac{1}{2} \cdot \frac{r_1 + 2\alpha_c^2}{\sigma_n^2 + 2\sigma_c^2}\right) \cdot I_0\left(\frac{\sqrt{2r_1} \cdot \alpha_c}{\sigma_n^2 + 2\sigma_c^2}\right) \quad (88)$$

and similarly,

$$f_{R_2}(R_2|S_{j_2}) = \frac{r_2}{(\sigma_n^2 + 2\sigma_j^2)} \cdot \exp\left(-\frac{1}{2} \cdot \frac{r_2 + 2\alpha_j^2}{\sigma_n^2 + 2\sigma_j^2}\right) \cdot I_0\left(\frac{\sqrt{2r_2} \cdot \alpha_j}{\sigma_n^2 + 2\sigma_j^2}\right) \quad (89)$$

Since R_1 and R_2 are independent random variables, the joint pdf of R_1 and R_2 is equal to the product of the individual pdfs:

$$f_{R_1 R_2}(r_1, r_2|l, S_{j_2}) = f_{R_1}(r_1|l) \cdot f_{R_2}(r_2|S_{j_2}) \quad (90)$$

$$\text{So } \Pr(R_1 < R_2|l, S_{j_2}) = \int_0^\infty \int_{r_1}^\infty f_{R_1} \cdot f_{R_2} dr_2 dr_1 = \int_0^\infty f_{R_1}(r_1|l) \cdot \left[\int_{r_1}^\infty f_{R_2}(r_2|S_{j_2}) dr_2 \right] dr_1 \quad (91)$$

For the inner integral,

$$\int_{r_1}^{\infty} f_{R_2}(r_2 | S_{j_2}) dr_2 = \int_{r_1}^{\infty} \frac{r_2}{\sigma_n^2 + 2\sigma_j^2} \cdot \exp\left[-\frac{r_2 + 2\alpha_j^2}{2(\sigma_n^2 + 2\sigma_j^2)}\right] \cdot I_0\left(\frac{\sqrt{2}r_2\alpha_j}{\sigma_n^2 + 2\sigma_j^2}\right) dr_2 \quad (92)$$

$$\text{Let } x = \frac{r_2}{\sqrt{\sigma_n^2 + 2\sigma_j^2}} \Rightarrow dx = \frac{dr_2}{\sqrt{\sigma_n^2 + 2\sigma_j^2}} \text{ and } \frac{r_1}{\sigma_n^2 + 2\sigma_j^2} = \frac{x \cdot \sqrt{\sigma_n^2 + 2\sigma_j^2}}{\sigma_n^2 + 2\sigma_j^2} \quad (93)$$

$$\text{Also to transform the lower limit of integration, when } r_2 = r_1, x = \frac{r_1}{\sqrt{\sigma_n^2 + 2\sigma_j^2}} \quad (94)$$

Using (92), (93), and (94) to (91), we get

$$\Pr(R_1 < R_2 | S_{j_2}) = \int_{\frac{r_1}{\sqrt{\sigma_n^2 + 2\sigma_j^2}}}^{\infty} x \cdot \exp\left(-\frac{x^2}{2} - \frac{\frac{2\alpha_j^2}{\sigma_n^2 + 2\sigma_j^2}}{2}\right) \cdot I_0\left(\frac{\sqrt{2} \cdot \alpha_j}{\sqrt{\sigma_n^2 + 2\sigma_j^2}} \cdot x\right) dx \quad (95)$$

Now compare the integral above with the Marcum's Q-function [2], [4]:

$$Q(a, \beta) = \int_{\beta}^{\infty} x \cdot \exp\left(-\frac{x^2 + a^2}{2}\right) \cdot I_0(ax) dx, \quad (96)$$

and notice that if we let

$$a = \frac{\alpha_j}{\sqrt{\sigma_n^2 + 2\sigma_j^2}}, \quad \beta = \frac{r_1}{\sqrt{\sigma_n^2 + 2\sigma_j^2}}$$

Then (95) is given by

$$Q(a, \beta) = Q\left(\frac{\sqrt{2\alpha_j^2}}{\sqrt{\sigma_n^2 + 2\sigma_j^2}}, \frac{\sqrt{r_1^2}}{\sqrt{\sigma_n^2 + 2\sigma_j^2}}\right). \quad (97)$$

Substituting (97) in (91), we get

$$\begin{aligned} \Pr(R_1 < R_2 | l, S_{j_2}) &= \int_0^\infty \frac{r_1}{\sigma_n^2 + 2\sigma_j^2} \cdot \exp\left(-\frac{r_1^2 + 2\alpha_c^2}{2(\sigma_n^2 + 2\sigma_j^2)}\right) \cdot I_0\left(\frac{\sqrt{2}r_1\alpha_c}{\sigma_n^2 + 2\sigma_j^2}\right) \\ &\quad \cdot Q\left(\frac{\sqrt{2\alpha_j^2}}{\sqrt{\sigma_n^2 + 2\sigma_j^2}}, \frac{\sqrt{r_1^2}}{\sqrt{\sigma_n^2 + 2\sigma_j^2}}\right) \end{aligned} \quad (98)$$

Consider the following identity[5]:

$$\begin{aligned} \int_0^\infty Q\left(\frac{a_2}{\sigma_2}, \frac{R_1}{\sigma_2}\right) \cdot \frac{R_1}{\sigma_1^2} \cdot \exp\left(-\frac{a_1^2 + R_1^2}{2\sigma_1^2}\right) \cdot I_0\left(\frac{a_1 R_1}{\sigma_1^2}\right) dR_1 = \\ \frac{\sigma_1^2}{\sigma_1^2 + \sigma_2^2} \cdot \left[1 - Q\left(\sqrt{\frac{a_1^2}{\sigma_1^2 + \sigma_2^2}}, \sqrt{\frac{a_2^2}{\sigma_1^2 + \sigma_2^2}}\right)\right] + \frac{\sigma_2^2}{\sigma_1^2 + \sigma_2^2} \cdot Q\left(\sqrt{\frac{a_2^2}{\sigma_1^2 + \sigma_2^2}}, \sqrt{\frac{a_1^2}{\sigma_1^2 + \sigma_2^2}}\right) \end{aligned} \quad (99)$$

If we let

$$\sigma_2 = \sqrt{\sigma_n^2 + 2\sigma_j^2}, \quad a_2 = \alpha_j \cdot \sqrt{2}, \quad R_1 = r_1, \quad \sigma_1 = \sqrt{\sigma_n^2 + 2\sigma_c^2}, \quad a_1 = \sqrt{2} \cdot \alpha_c$$

then (99) can be used to evaluate (98) with the result

$$\begin{aligned} \Pr(R_1 < R_2 | l, S_{j_2}) &= \frac{\sigma_n^2 + 2\sigma_c^2}{2(\sigma_n^2 + \sigma_c^2 + \sigma_j^2)} \cdot \left[1 - Q\left(\sqrt{\frac{\alpha_c^2}{\sigma_n^2 + \sigma_c^2 + \sigma_j^2}}, \sqrt{\frac{\alpha_j^2}{\sigma_n^2 + \sigma_c^2 + \sigma_j^2}}\right) \right] + \\ &+ \frac{\sigma_n^2 + 2\sigma_j^2}{2(\sigma_n^2 + \sigma_c^2 + \sigma_j^2)} \cdot Q\left(\sqrt{\frac{\alpha_j^2}{\sigma_n^2 + \sigma_c^2 + \sigma_j^2}}, \sqrt{\frac{\alpha_c^2}{\sigma_n^2 + \sigma_c^2 + \sigma_j^2}}\right) \end{aligned} \quad (100)$$

Using (23) and (24), we get

$$\begin{aligned} \Pr(R_1 < R_2 | l, S_{j_2}) &= \frac{1 + \xi_c}{2 + \xi_c + \xi_j} \cdot \left[1 - Q\left(\frac{\sqrt{2\rho_c}}{\sqrt{2 + \xi_c + \xi_j}}, \frac{\sqrt{2\rho_j}}{\sqrt{2 + \xi_c + \xi_j}}\right) \right] + \\ &+ \frac{1 + \xi_j}{2 + \xi_c + \xi_j} \cdot Q\left(\frac{\sqrt{2\rho_j}}{\sqrt{2 + \xi_c + \xi_j}}, \frac{\sqrt{2\rho_c}}{\sqrt{2 + \xi_c + \xi_j}}\right) \end{aligned} \quad (101)$$

We can now use the identity [5]:

$$Q(a, \beta) = 1 - Q(\beta, a) + \exp\left(-\frac{a^2 + \beta^2}{2}\right) \cdot I_0(a, \beta) \quad (102)$$

in (101) to get

$$\begin{aligned} \Pr(R_1 < R_2 | l, S_{j_2}) &= Q\left(\frac{\sqrt{2\rho_j}}{\sqrt{2 + \xi_c + \xi_j}}, \frac{\sqrt{2\rho_c}}{\sqrt{2 + \xi_c + \xi_j}}\right) \\ &- \frac{1 + \xi_c}{2 + \xi_c + \xi_j} \cdot \exp\left(-\frac{\rho_c + \rho_j}{2 + \xi_c + \xi_j}\right) \cdot I_0\left(\frac{2\sqrt{\rho_c\rho_j}}{2 + \xi_c + \xi_j}\right) \end{aligned} \quad (103)$$

D. $\Pr(R_1 < R_2 | l, S_{j_1}, S_{j_2})$

This probability of error is obtained from $\Pr(R_1 < R_2 | l, S_{j_2})$ by altering the signal in branch one to include the jammer tone S_{j_1} . As before, a_c^2 is replaced with $a_c^2 + a_j^2 + 2a_c a_j \cos(\theta_j)$. We must then integrate twice to eliminate the dependence on the fading parameters. The phase angle θ requires a third integration. However, the integrations cannot be evaluated analytically. The triple numerical integration is time consuming. As will be explained later, an effort is made to approximate θ so as to avoid the third integration.

The $\Pr(R_1 < R_2 | l, S_{j_2})$ for a non-fading channel is given in [6] as

$$\Pr(R_1 < R_2 | l, S_{j_2}) = \frac{1}{2} \left[1 - Q\left(\sqrt{\frac{a_c^2}{\sigma_n^2}}, \sqrt{\frac{a_j^2}{\sigma_n^2}}\right) + Q\left(\sqrt{\frac{a_j^2}{\sigma_n^2}}, \sqrt{\frac{a_c^2}{\sigma_n^2}}\right) \right]. \quad (104)$$

Using (102), we get

$$1 - Q\left(\sqrt{\frac{a_c^2}{\sigma_n^2}}, \sqrt{\frac{a_j^2}{\sigma_n^2}}\right) = Q\left(\sqrt{\frac{a_j^2}{\sigma_n^2}}, \sqrt{\frac{a_c^2}{\sigma_n^2}}\right) - \exp\left(-\frac{a_c^2 + a_j^2}{2\sigma_n^2}\right) \cdot I_0\left(\frac{a_c \cdot a_j}{\sigma_n^2}\right) \quad (105)$$

and substituting (105) into (104), we get

$$\Pr(R_1 < R_2 | l, S_{j_2}) = Q\left(\sqrt{\frac{a_j^2}{\sigma_n^2}}, \sqrt{\frac{a_c^2}{\sigma_n^2}}\right) - \frac{1}{2} \exp\left(-\frac{a_c^2 + a_j^2}{2\sigma_n^2}\right) \cdot I_0\left(\frac{a_c \cdot a_j}{\sigma_n^2}\right). \quad (106)$$

Now, replacing a_c^2 with $a_c^2 + a_j^2 + 2a_c a_j \cos(\theta)$, we get

$$\begin{aligned}
\Pr(R_1 < R_2 | l, S_{j_1}, S_{j_2}, a_c, a_j, \theta) = \\
Q\left(\sqrt{\frac{a_j^2}{\sigma_n^2}}, \sqrt{\frac{a_c^2 + a_j^2 + 2a_c a_j \cos(\theta)}{\sigma_n^2}}\right) - \frac{1}{2} \exp\left(-\frac{a_c^2 + 2a_j^2 + 2a_c a_j \cos(\theta)}{2\sigma_n^2}\right) \cdot \\
I_0\left(\frac{a_j}{\sigma_n} \cdot \sqrt{\frac{a_c^2 + a_j^2 + 2a_c a_j \cos(\theta)}{\sigma_n^2}}\right)
\end{aligned} \tag{107}$$

The dependence on a_c , a_j , and θ must be removed by multiplying (107) by the Ricean pdfs for the signal and jammer tones, respectively, and by the pdf for θ and then integrating over a_c , a_j , and θ . As previously mentioned, this must be done numerically and can be a computationally intensive operation. In any event, the problem at hand has been "solved" in the sense expressed in [7]:

In many cases we shall consider the solution found if we can express it in terms of one or more integrals, even if the integration can only be performed by expanding in series (or computing numerically). This is called 'reducing to quadratures', a phrase by which the mathematician symbolically washes his hands of the remainder of the task of finding the solution.

This completes the analysis of the receiver performance for independent multitone jamming. The final form of the equations that must be evaluated are summarized in the appendix, equations B.6 through B.12. Many of these equations are also used for the analysis of band multitone jamming, which is addressed in the next chapter.

VI. FH/MFSK RECEIVER PERFORMANCE WITH BAND MULTITONE INTERFERENCE

Band multitone jamming implies that the multiple, equal power jamming tones are distributed randomly across the entire frequency-hopped bandwidth with a specific number of jamming tones placed in a frequency-hop bin given that a particular hop bin is jammed. For worst case band multitone jamming, the worst probability of bit error is obtained when at most a single interfering tone exists at one of the M possible orthogonal signaling frequencies in a specific FH band. This section considers the general case of a jammer using L jamming tones per hop bin with $1 \leq L \leq M$. We require the probability that the jammer places a set of L tones within the signal frequency-hop bin. This probability is derived by considering the following numerical example. Suppose that we have a total of 10 jammer tones ($q = 10$), and two jamming tones per jammed bin ($L = 2$). Suppose that the number of hop bins is 30 ($N=30$). The jammer tones are grouped into $q/L = 5$ sets, each set composed of two tones. Now, the probability that one of the five sets exists in one of the $N = 30$ hop bins is $5/30$. In the general case, the probability that the hop bin is jammed is

$$\Pr(\text{bin jammed}) = \frac{q/L}{N} = \frac{q}{N \cdot L} . \quad (108)$$

The probability that the hop bin is not jammed is

$$\Pr(\text{bin not jammed}) = 1 - \frac{q}{N \cdot L} . \quad (109)$$

From the total probability law, we find that the overall probability of error is:

$$\begin{aligned}
\Pr(\text{error}) &= \Pr(L, L \geq 1) \cdot P_s(L, L \geq 1) + \Pr(L = 0) \cdot P_s(L = 0) \\
&= \frac{q}{N \cdot L} \cdot P_s(L, L \geq 1) + \left(1 - \frac{q}{N \cdot L}\right) \cdot P_s(L = 0)
\end{aligned} \tag{110}$$

The probability of symbol error when a hop bin is not jammed, $P_s(L = 0)$, is the same as the probability of symbol error for noncoherent MFSK and no tone interference

$$P_s(L = 0) \leq (M - 1) \cdot \Pr(R_1 < R_2 | l). \tag{111}$$

This non-jamming case must be considered in order to account for every possible jamming scenario.

The probability of symbol error when a hop bin is jammed is found in (38) to be ($L \geq 1$):

$$\begin{aligned}
P_s(L) &\leq \frac{L}{M} \cdot \left[(L - 1) \cdot \Pr(R_1 < R_2 | l, S_{j_1}, S_{j_2}) + (M - L) \cdot \Pr(R_1 < R_2 | l, S_{j_1}) \right] + \\
&\quad + \left(1 - \frac{L}{M}\right) \cdot \left[L \cdot \Pr(R_1 < R_2 | l, S_{j_2}) + (M - L - 1) \cdot \Pr(R_1 < R_2 | l) \right]
\end{aligned} \tag{112}$$

Hence, combining (110), (111) and (112), we obtain the probability of symbol error when ($L \geq 1$) as

$$\begin{aligned}
Ps(L) \leq & \frac{q}{N \cdot L} \cdot \left\{ \frac{L}{M} \cdot \left[(L-1) \cdot \Pr(R_1 < R_2 | l, S_{j_1}, S_{j_2}) + (M-L) \cdot \Pr(R_1 < R_2 | l, S_{j_1}) \right] + \right. \\
& \left. \left(1 - \frac{L}{M} \right) \cdot \left[L \cdot \Pr(R_1 < R_2 | l, S_{j_2}) + (M-L-1) \cdot \Pr(R_1 < R_2 | l) \right] \right\} \\
& \left(1 - \frac{q}{N \cdot L} \right) \cdot \left((M-1) \frac{1}{2 + \xi_c} \cdot \exp\left(-\frac{\rho_c}{2 + \xi_c}\right) \right).
\end{aligned}
\tag{113}$$

The individual probabilities appearing in (113) are identical to the ones found in the last chapter, and are given in (58), (79), (103), and (107). The difference from the independent multitone interference is that L is fixed.

This completes the analysis of the receiver performance for band multitone jamming. The final form of the equation that must be evaluated is given in the appendix as equation B.13. In the next chapter, numerical results are obtained for receiver performance with both band and independent multitone jamming.

VII. NUMERICAL RESULTS

The performance of the FH/MFSK receiver is investigated as a function of the ratio of the information signal power to the total interference power, $\frac{P_c}{P_{j_r}}$. Worst case performance is approximated by selecting q as the largest integer value between 1 and the ratio $\frac{P_{j_r}}{P_c}$. For non-worst-case performance, we select $q=100$.

The non-fading, Ricean, or Rayleigh fading channel for the signal and/or the jammer tones is modeled by appropriately selecting the values of the corresponding direct-to-diffuse power ratios, $\frac{a_c^2}{2\sigma_c^2}$ and $\frac{a_j^2}{2\sigma_j^2}$. A large ratio value implies little fading, a value of 10 implies Ricean fading, and a very small value implies Rayleigh fading. Due to programming necessities and in order to avoid divisions by zero, we use a ratio equal to 10^{-9} to simulate Rayleigh fading. For purposes of numerical computation, all curves are obtained with $E_b/N_0 = 13.35$ dB and $N=1000$. The zero thermal noise curve is also plotted in each figure to validate the results since this provides an upper bound. For band multitone interference with a single interfering tone per hop and zero thermal noise, the probability of bit error is equal to [8]

$$P_b = \frac{q}{N} \left[\frac{1}{2} u \left(\frac{P_{j_r}}{q} - P_c \right) \right], \quad (114)$$

while for independent multitone interference with zero thermal noise, the probability of bit error for FH/BFSK is [9]

$$P_b = \frac{q}{2N} \left(1 - \frac{q-1}{2N-1} \right) \cdot \frac{1}{2} u \left(\frac{P_{J_T}}{q} - P_c \right) + \frac{q}{2N} \left(\frac{q-1}{2N-1} \right) \frac{1}{\pi} \cos^{-1} \left(\sqrt{\frac{qP_c}{4P_{J_T}}} \right) \cdot u \left(\frac{P_{J_T}}{q} - \frac{P_c}{4} \right). \quad (115)$$

A. BAND MULTITONE INTERFERENCE

The performance of FH/BFSK with band multitone interference when the information signal is essentially unaffected by channel fading ($a^2_c / 2\sigma^2_c = 1000$) with $M=2$ and $M=8$, respectively is shown in Figures 2 and 3. L successively takes the values 1 and 2 in Figure 2 and the values 1, 4, and 8 in Figure 3. Performance is computed for both $q = 100$ and worst case q . When $P_j \geq P_c$, or equivalently $\frac{P_c}{P_{j_T}} \leq -20\text{dB}$ and $q=100$, the worst probability of bit error is obtained for at most a single interfering tone at one of the M possible orthogonal signaling frequencies ($L=1$). For the region where $P_c \geq P_j$, the worst case performance is obtained when all signal tones are jammed ($L=M$). Hence, a jammer whose power P_j is guaranteed to exceed the signal power will do more harm with just one tone per bin. However, a jammer with P_j guaranteed to be less than the power of a signal tone, will do more harm by jamming all M tones of a bin. For worst case q , the worst performance is obtained when $L=1$ for all power ratios.

The non-fading signal case for $M=2$ with all three possibilities of jammer tones fading is shown in Figure 4. The results are the same as those in [1]. When $P_j \geq P_c$ or equivalently $\frac{P_c}{P_{j_T}} \leq -20\text{dB}$ and $q=100$, the difference in performance is trivial regardless of whether or not the jammer tones are affected by the fading nature of the channel, even

when the jammer tones experience Rayleigh fading. On the other hand, when $P_c \geq P_j$, or equivalently $\frac{P_c}{P_{j_T}} \geq -20\text{dB}$, the interference tones that experience Rayleigh fading yield the poorest performance. For the worst case q , the difference is trivial for the entire range of signal-to-jammer power ratios. Figure 4 is identical to the figure we get if we use the exact result equations. In fact, the individual probabilities of bit error used in the exact result, as they are described in [1], are identical to those obtained with the union bound for the $M=2$ case. So $M=2$ will not be treated again by itself since it can convey no more information. It is important that for $M=2$ the simpler union bound equations provide the exact result.

The non-fading signal case for $M=8$ is shown in Figures 5 and 6 for $q=100$ and worst case q respectively. The curves obtained for the exact result and the union bound are identical and practically indistinguishable from each other. The previous phenomenon with regard to the effect of fading interference tones deduced from Figure 4 is also obvious here, but it is even more pronounced, with the non-fading and Rayleigh fading curves differing by 5dB.

The Ricean fading signal case for $q=100$ and worst case q is shown in Figures 7 and 8 respectively, where the exact and approximate solution's curves obtained for $M=8$ are compared. In Figure 7, we notice that the union bound curves are almost identical to the exact result ones and only in the region where $\frac{P_c}{P_{j_T}} \geq -10\text{dB}$ do they appear to have a constant difference of $1.38 \cdot 10^{-4}$. In Figure 8, the union bound curves behave as expected, being practically indistinguishable from the exact result ones for $P_c \leq P_{j_T}$, while in the opposite case they appear to have a slight difference with a maximum value equal to $1.38 \cdot 10^{-4}$. The union bound curves again work as an upper bound on the probability of bit error.

Summarizing the results up to this point, since the differences detected are trivial ones, for all practical purposes we infer that for M even larger than eight, we can easily

resort to the union bound equations to estimate the probability of bit error when the signal tones are either not affected at all by the fading channel or the signal tones experience Ricean fading.

The exact result and the union bound curves for a Rayleigh fading channel affecting the signal tones and the three possible cases of fading conditions for the jammer tones are shown in Figure 9. The difference between the two groups of curves attains a maximum value equal to 0.0038. This difference between the exact and union bound curves is the greatest noticed up to this point. The union bound curves still act as a bound, being higher than the exact result ones, but the accuracy is questionable. This is examined further in the following figures where we determine if increasing the number of symbols M causes a decrease in the probability of error as should normally happen.

The non-fading and Ricean fading signal curves in conjunction with every possible fading situation of the jammer tones is displayed in Figures 10 through 14. The value of M is sequentially changed, taking the values 2, 4, and 8. In these figures, no anomaly is detected, and the curves behave correctly in all cases with the probability of error decreasing as the number of symbols M increases. However, the next three figures, Figures 15, 16, and 17, display the Rayleigh fading signal case in conjunction with all three possible fading conditions of the jammer tones. In all cases the results obtained are incorrect. The union bound still acts as a bound, but the probability of error erroneously increases as M increases.

Summarizing the union bound approach for band multitone interference, we see that for the non-fading and the Ricean fading signal case, the union bound approach gives very accurate results which are perfect in the first case and deteriorate some in the second though still providing acceptable accuracy. However, when the signal tones experience Rayleigh fading, the union bound approach should be avoided because the accuracy obtained is not sufficient. From a computational point of view, the union bound approach is far simpler than the exact approach. The exact approach equations include joint pdfs of two random variables expressed with double integrals. On the contrary, the

union bound equations are expressed as the sum of individual pdfs of one random variable and thus they are expressed in terms of one or more integrals.

B. INDEPENDENT MULTITONE INTERFERENCE

In independent multitone interference, the number of tones existing per frequency hop bin can vary from zero to M , where it equates to the number of signal tones. As mentioned before, the calculation of the probability of error here is time consuming due to the inability to further simplify the solution which contains three integrations. However, one integration is eliminated for the case where either the signal or the jammer tones are not affected by the fading channel, and two integrations can be eliminated for the case where both the signal and jammer tones are non-fading.

The $M=2$ case for a non-fading signal and various jammer fading cases when we have independent multitone interference is shown in Figure 18. As with band multitone interference, the results obtained for $M=2$ are identical with the ones given by the exact solution. This is because the exact solution equations, described in [1], again coincide with the union bound for $M=2$, enabling us again to use the union bound with perfect accuracy. As in band multitone interference, we notice the performance degradation from the non-fading jammer case to the Rayleigh fading jammer case when $P_c \geq P_j$.

The non-fading signal case for $M=8$ is shown in Figure 19. It is obvious that the union bound approach is a valuable tool in this case since the exact result approach requires very complicated probabilistic equations with the complexity further increased as M increases. However, the union bound approach provides us with a concise expression for any value of M . The only means of comparing the curves obtained here with a pre-existing result is to get a feeling from the comparable ones obtained for band multitone interference case bearing in mind the result obtained in [1], that the probability of error for the band multitone interference is poorer than for independent multitone interference. In fact, comparing Figures 5 and 19, we see that they have the same shape, differing by a

factor of roughly eight. Also, comparing Figures 4 and 18, we see that they differ by a factor of roughly equal two. The difference between band and independent multitone interference is roughly equal to M .

Figure 19 is characterized by the phenomenon previously described. For $P_e \geq P_j$ a channel with no fading of the interference tones provides an advantage of up to 5dB over one with Rayleigh fading.

The Ricean fading signal case for $M=2$ with all three possibilities of fading of the jammer tones is displayed in Figure 20. As for non-fading signal tones, when $q=100$ we notice a difference in performance for the non-fading and Rayleigh fading jammer tones when $P_e \geq P_j$. That difference, however, is now less pronounced. For the worst case q , the difference between the respective curves is again trivial. Comparing this figure with Figure 3, we again notice that the probability of error is less by a factor of roughly two.

The Ricean fading signal case for $M=8$ with all three possibilities of fading of the jammer tones is displayed in Figure 21. Comparing this figure with Figure 7, we notice that the probability of error difference is eight. This confirms the previous observation that the decrease in probability of error when we shift from band to independent multitone interference is roughly equal to M .

The Rayleigh fading signal case for $M=2$ and $M=8$ with non-fading interference for $q = 100$ and worst case q is shown in Figure 22. The obvious problem is the same as the one observed for band multitone interference. The accuracy achieved is not sufficient and predicts an increase in the probability of bit error for an increase in the number of symbols M . Thus, the union bound approach should be avoided when the signal experiences Rayleigh fading.

The remaining figures, Figures 23, 24, 25, and 26, show the results of approximating θ rather than integrating over all of its possible values. Remember that by θ we denote the difference between the phase of the signal and the phase of the jammer tones. This is modeled as a uniformly distributed random variable over $[0, 2\pi]$. As mentioned before, in the beginning of this section, for the case of more than one jammer

tone per frequency hop bin, we must perform three numerical integrations in order to calculate the probability of error: one for the amplitude of the signal tone fading, one for the amplitude of the jammer tone fading, and one for the angle θ . To this must be added the embedded calculation of the Marcum's Q-function that is also defined in integral form. It would be very convenient to find a way to eliminate one numerical integration. In fact, the integration over θ was experimentally found to be the most time consuming one. After trying different angle values to get an accurate approximation, it is found that for $\theta = \frac{7}{10} \cdot \pi$ the approximation is so good that the difference between the exact and approximated traces can barely be detected. The exact and approximated curves for a non-fading signal and various fading of the jammer tones for $M=2$ and $M=8$, respectively, are shown in Figures 23 and 24. The exact and approximated curves for a Ricean fading signal and various fading of the jammer tones for $M=2$ and $M=8$, respectively, are shown in Figures 25 and 26. This approximation results in a significant reduction in computational complexity and time.

VIII. CONCLUSION

From a probabilistic performance point of view, the results obtained verify those of [1] that when $P_j \geq P_c$ the effect of fading jammer tones is very small when the signal tones are not affected by fading. When $P_c > P_j$ performance is poorer when the interference tones experience fading. When the information signal experiences fading, the effect of fading interference tones is less.

With regard to the union bound approach, it is shown to be very accurate for non-fading or Ricean fading signal tones, while for Rayleigh fading signals its use should be avoided.

The application of the union bound for the Ricean fading signal in the case of independent multitone interference for $M=2$ and $M=8$, that was not treated in [1], shows that the probability of error advantage when the jammer uses independent multitone interference instead of band multitone interference is equal to a factor of M . Hence, when $M = 8$, independent multitone interference gives probabilities of error eight times less than does band multitone interference.

In case of the independent multitone interference, the calculations involved can be much simplified if instead of integrating over all possible values of θ we let $\theta = \frac{7}{10} \cdot \pi$, thus eliminating the most time-consuming integration.

In summary, the union bound approach taken in this thesis not only simplifies the computational complexity involved in obtaining numerical results, but also allows us to analytically evaluate situations that are not amenable to solution using an exact approach. The principle drawback is the breakdown of the union bound approach when the signal experiences Rayleigh fading.

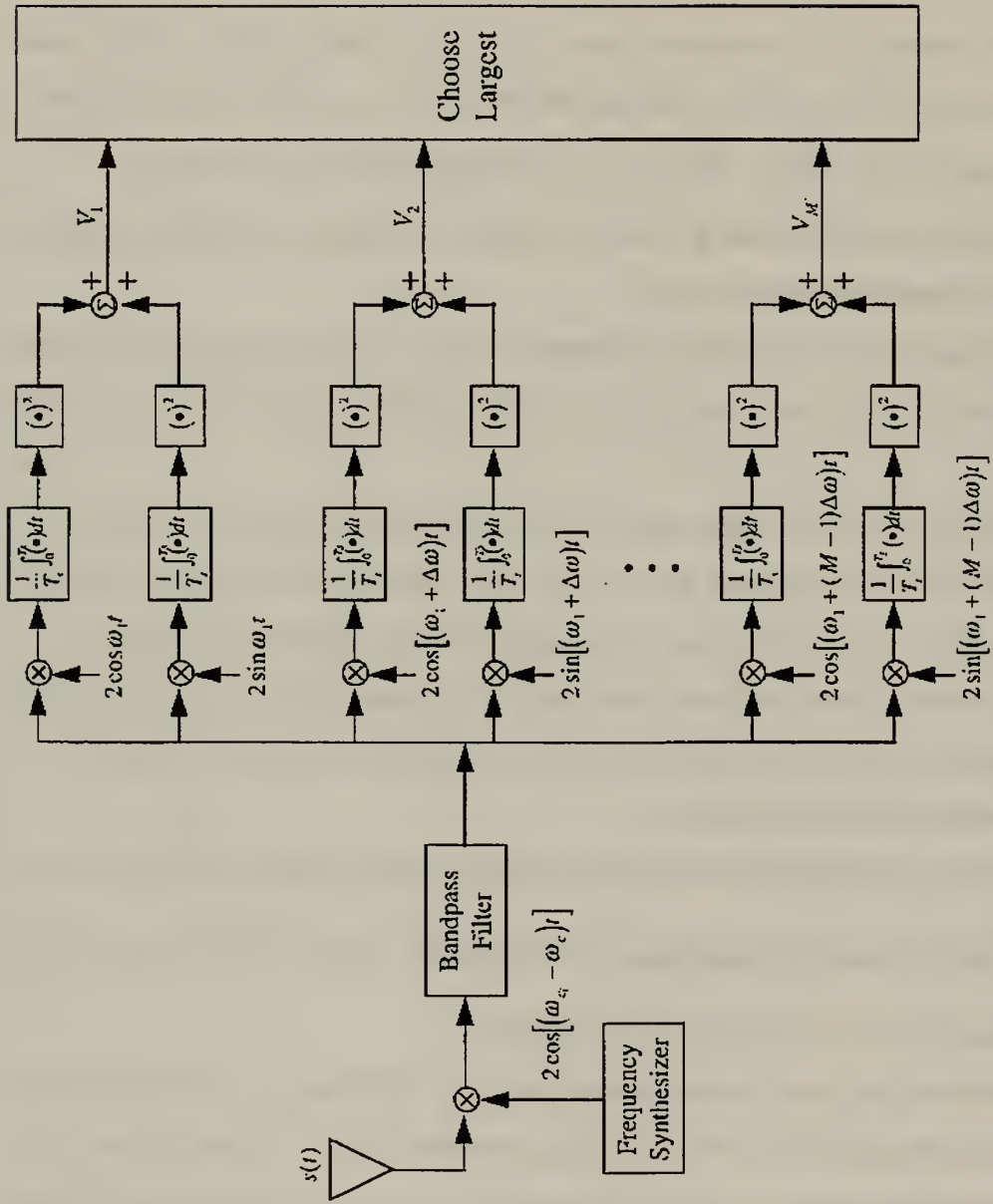


Figure 1: Noncoherent FH/MFSK Receiver

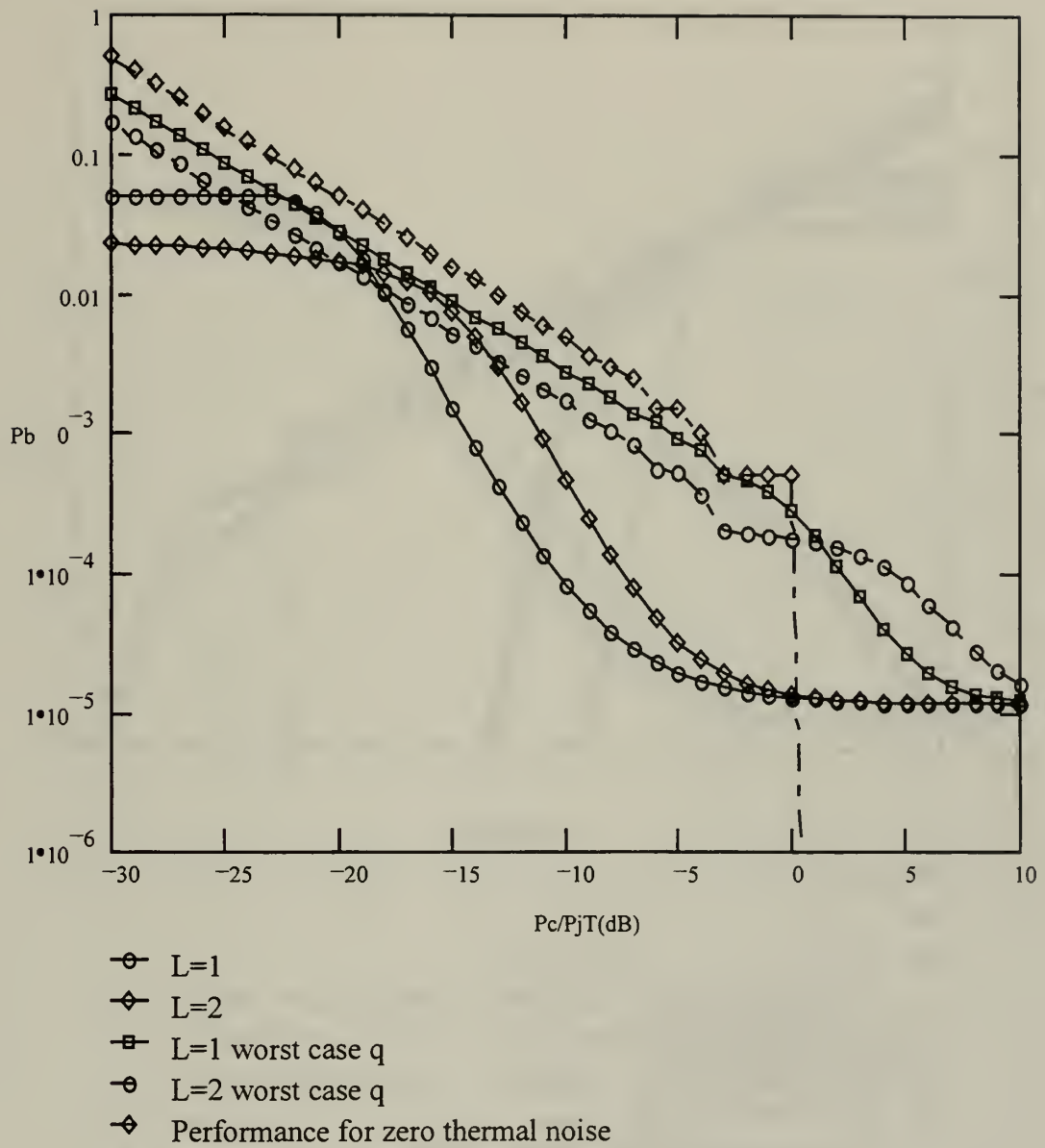


Figure 2: Performance of a FH/BFSK noncoherent receiver with essentially no information signal fading for band multitone interference with various conditions of fading of the multiple interference tones for $L=1$ and $L=2$.

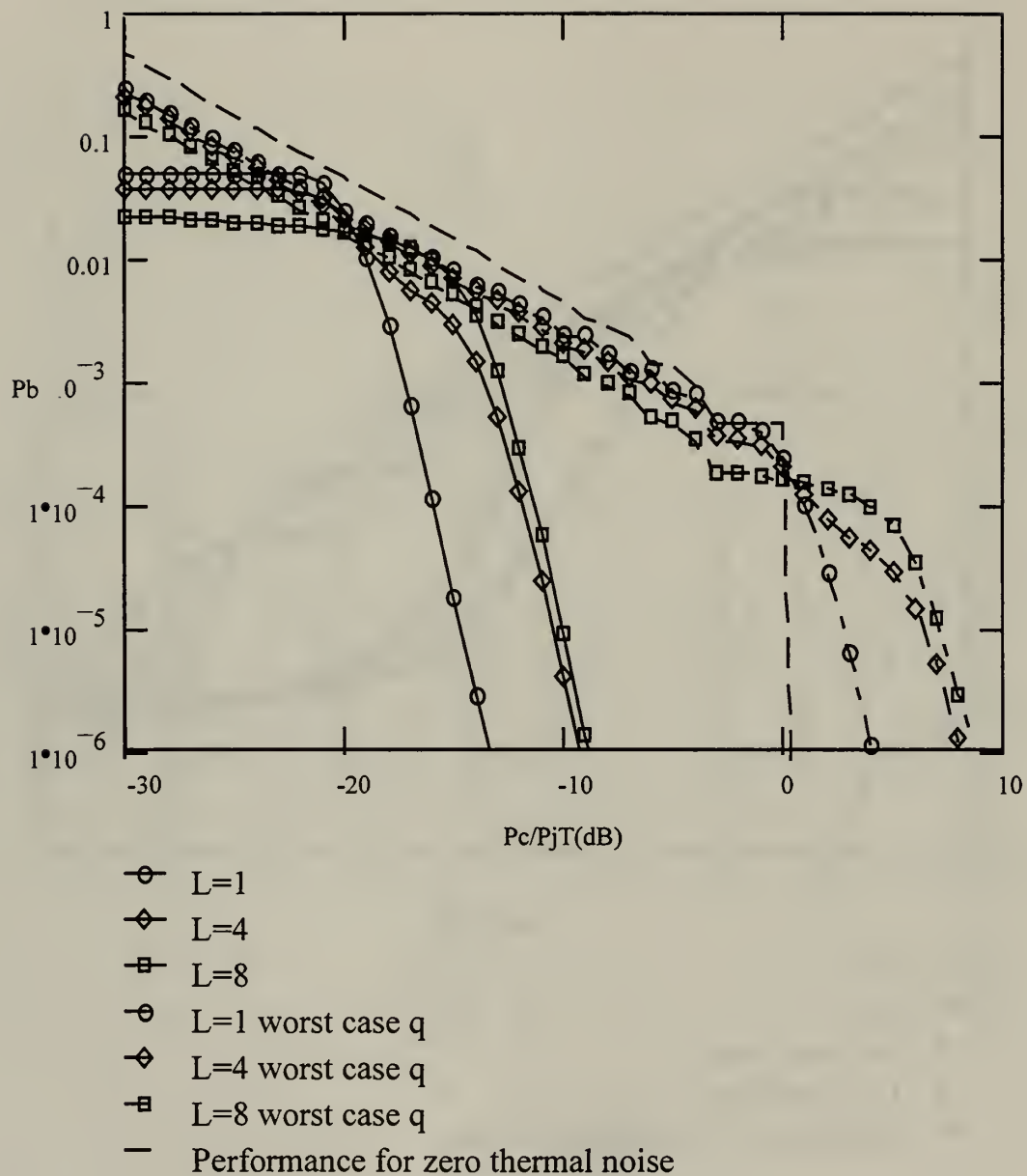


Figure 3: Performance of a FH/8FSK noncoherent receiver with essentially no information signal fading for band multitone interference with various conditions of fading of the multiple interference tones for $L=1$, $L=4$, and $L=8$.

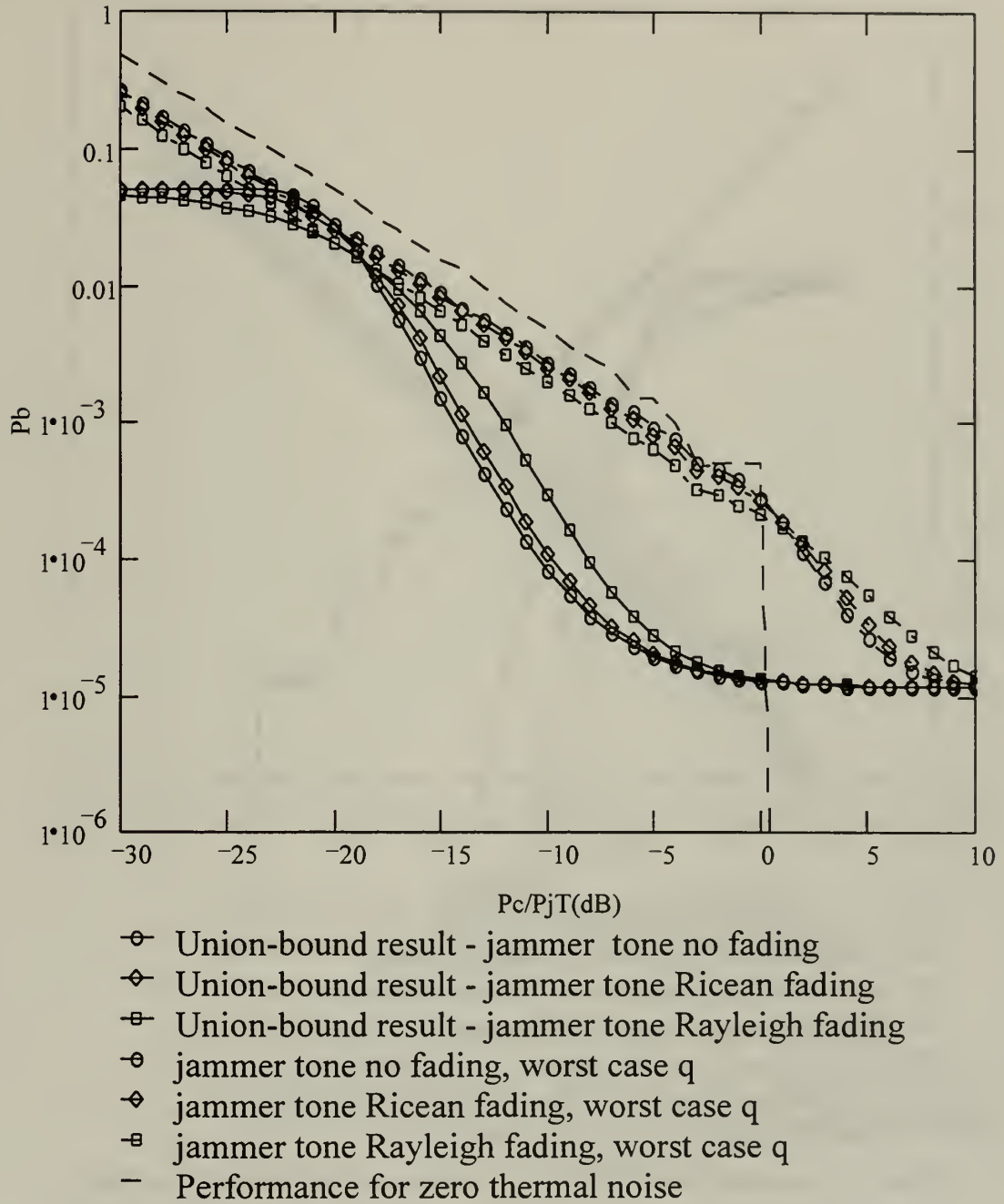


Figure 4: Performance of a FH/BFSK noncoherent receiver with essentially no information signal fading for band multitone interference with various conditions of fading of the multiple interference tones. The results are identical with those obtained using the exact result equations.

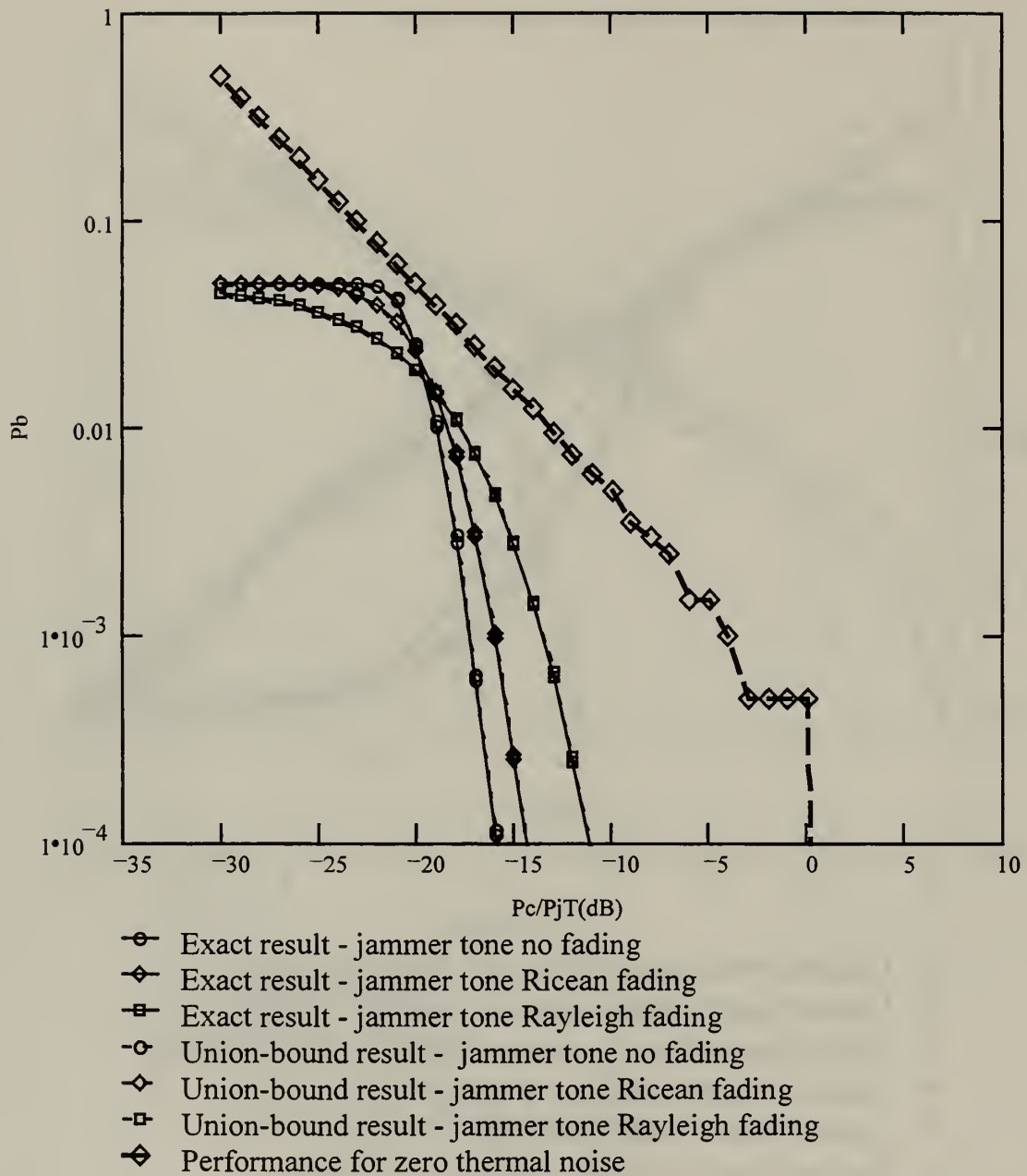


Figure 5: Performance of a FH/8FSK noncoherent receiver with essentially no information signal fading for band multitone interference with various conditions of fading of the multiple interference tones, $q = 100$, using both the exact result and the union bound equations. The curves obtained are identical and practically indistinguishable.

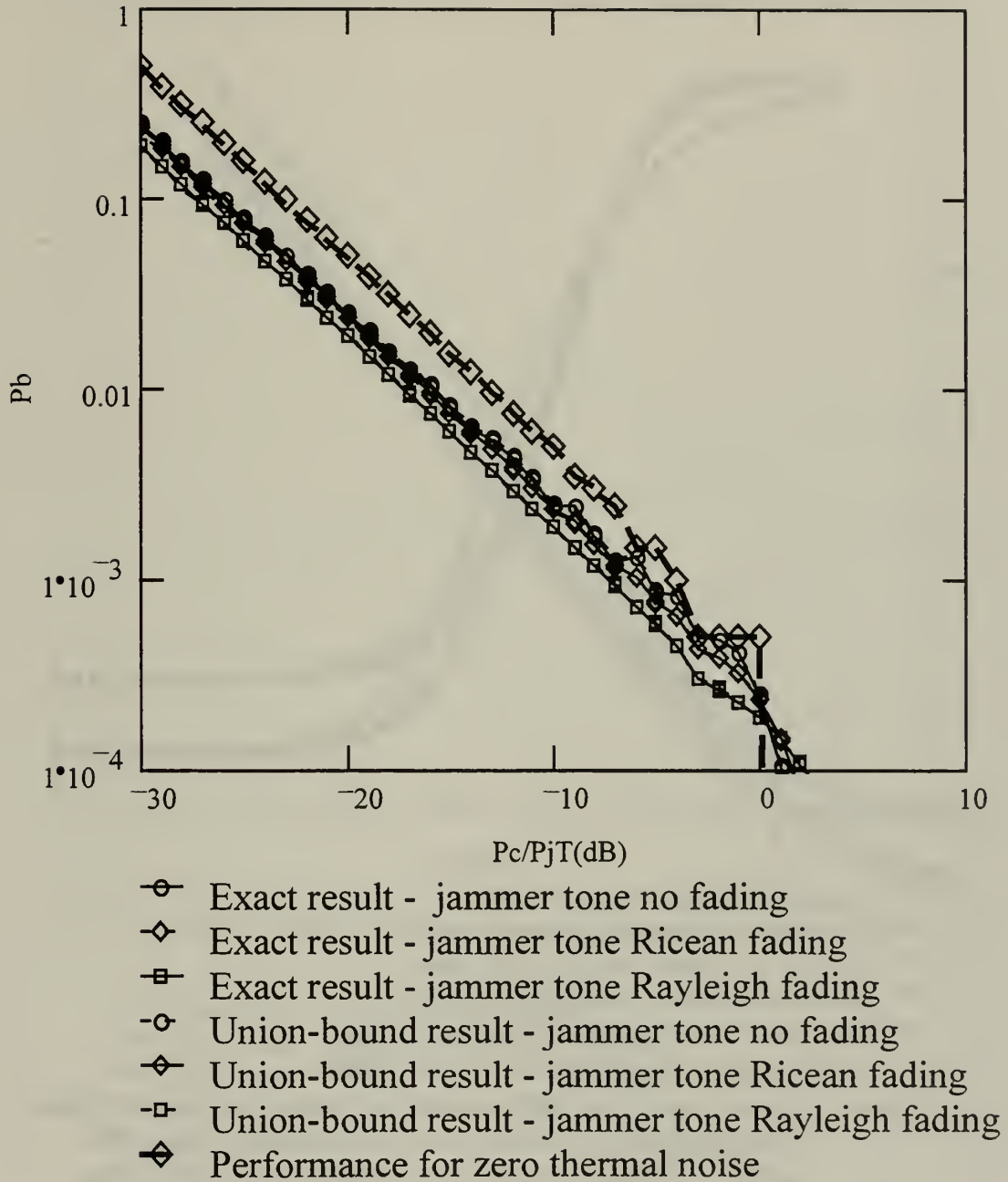


Figure 6: Performance of a FH/8FSK noncoherent receiver with essentially no information signal fading for band multitone interference with various conditions of fading of the multiple interference tones, q_{wc} , using both the exact result and the union bound equations. The curves obtained are identical and practically indistinguishable.

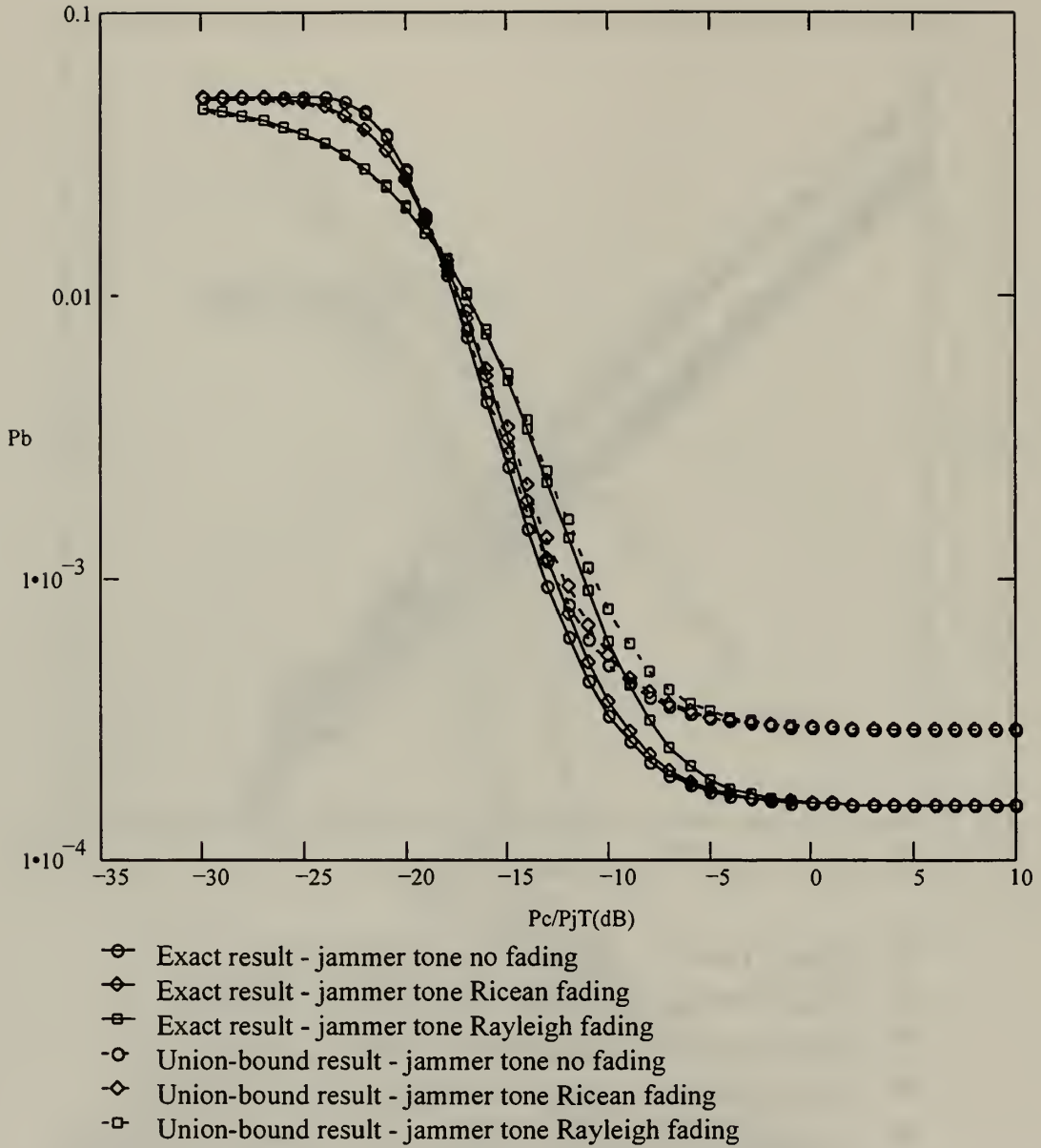


Figure 7: Performance of an 8FSK noncoherent receiver with Ricean fading of the information signal for band multitone interference with various conditions of fading of the multiple interference tones, $q = 100$, using both the exact result and the union bound equations. The union bound curves behave as expected, being a little higher than the exact solution ones. For $\frac{P_c}{P_{jT}} > -10$ dB we lose a little bit of accuracy as the union-bound curves have the same shape with the exact result curves but they have a constant difference of $1.36 \cdot 10^{-4}$. As in the $M=2$ case, **there is no essential difference between no fading, Ricean fading and Rayleigh fading of the jamming tones, for $P_{jT} \geq P_c$.**

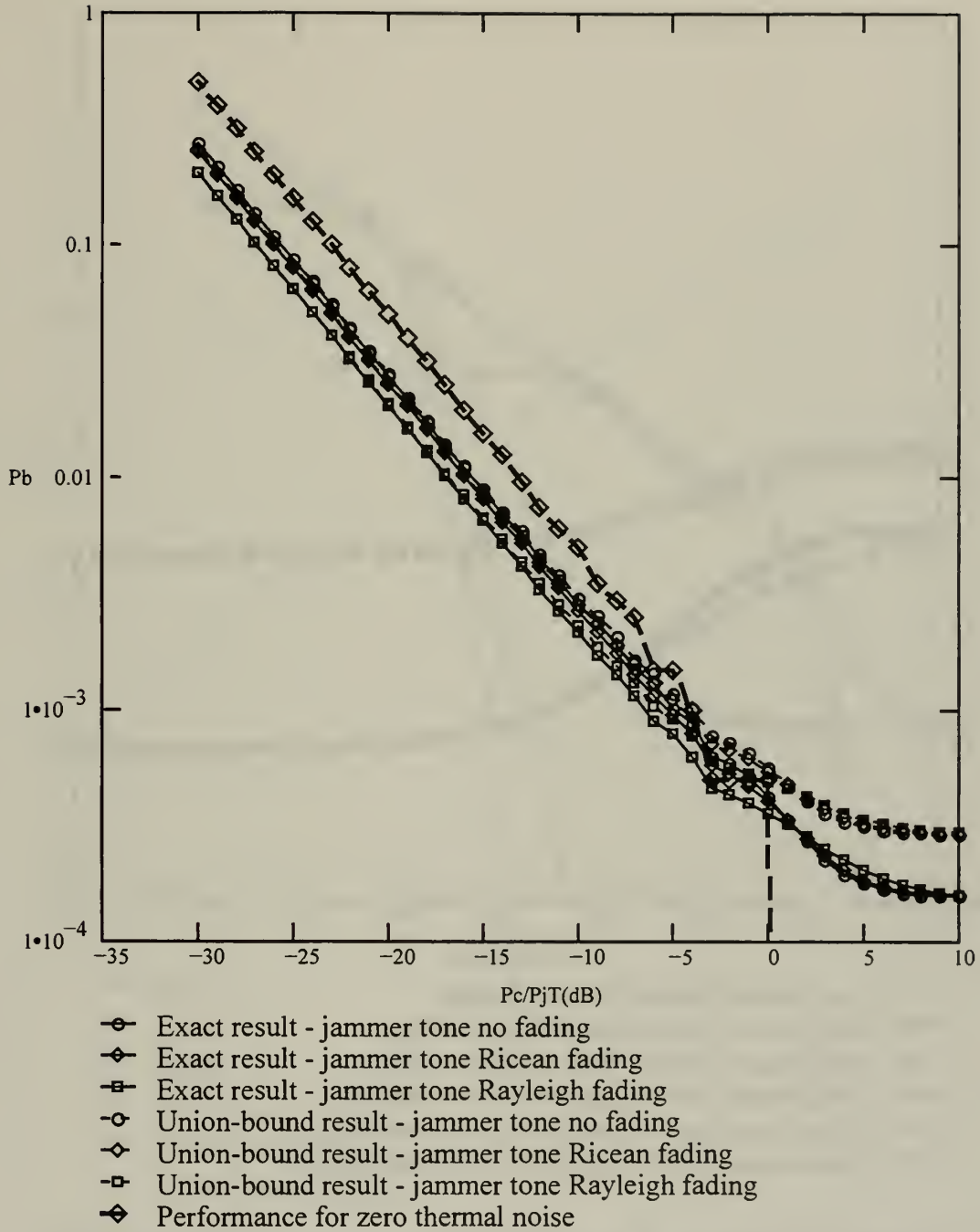


Figure 8: Performance of an 8FSK noncoherent receiver with Ricean fading of the information signal for band multitone interference with various conditions of fading of the multiple interference tones, q_{wc} , using both the exact result and the union bound equations. The union bound curves behave as expected, being practically indistinguishable from the exact result equations for $P_c < P_{jT}$ while for $P_c > P_{jT}$ they appear a little bit higher, having a maximum difference of $1.34 \cdot 10^{-4}$.

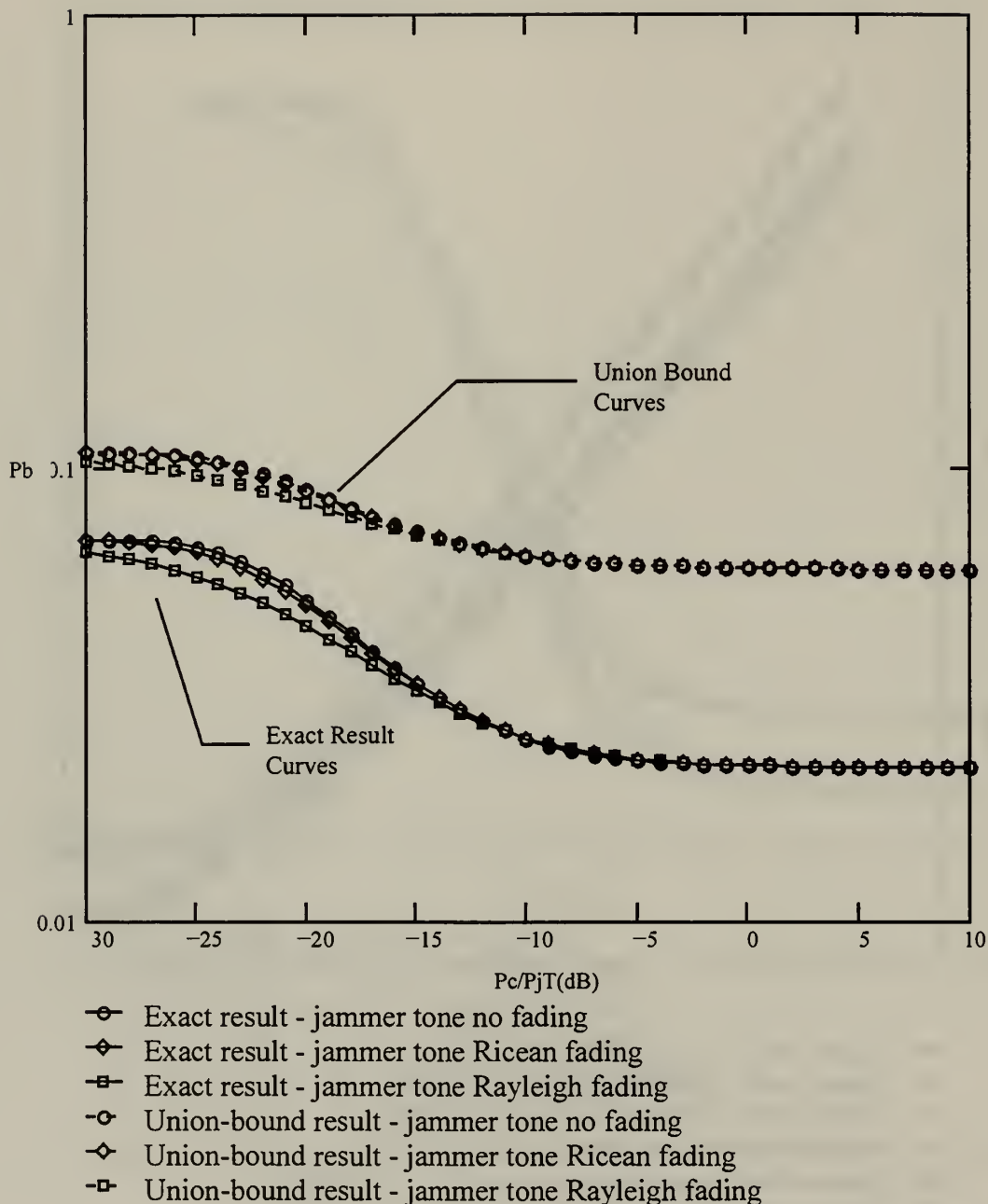


Figure 9: Performance of an 8FSK noncoherent receiver with Ricean fading of the information signal for band multitone interference with various conditions of fading of the multiple interference tones, $q = 100$, using both the exact result and the union bound equations. Again the fading behaviour of the jammer tone is irrelevant to the probability of error. The union bound curves have the same form as the ones from the exact result, but appear to display the biggest error than in any case treated up to this point, an error having a maximum equal to 0.038.

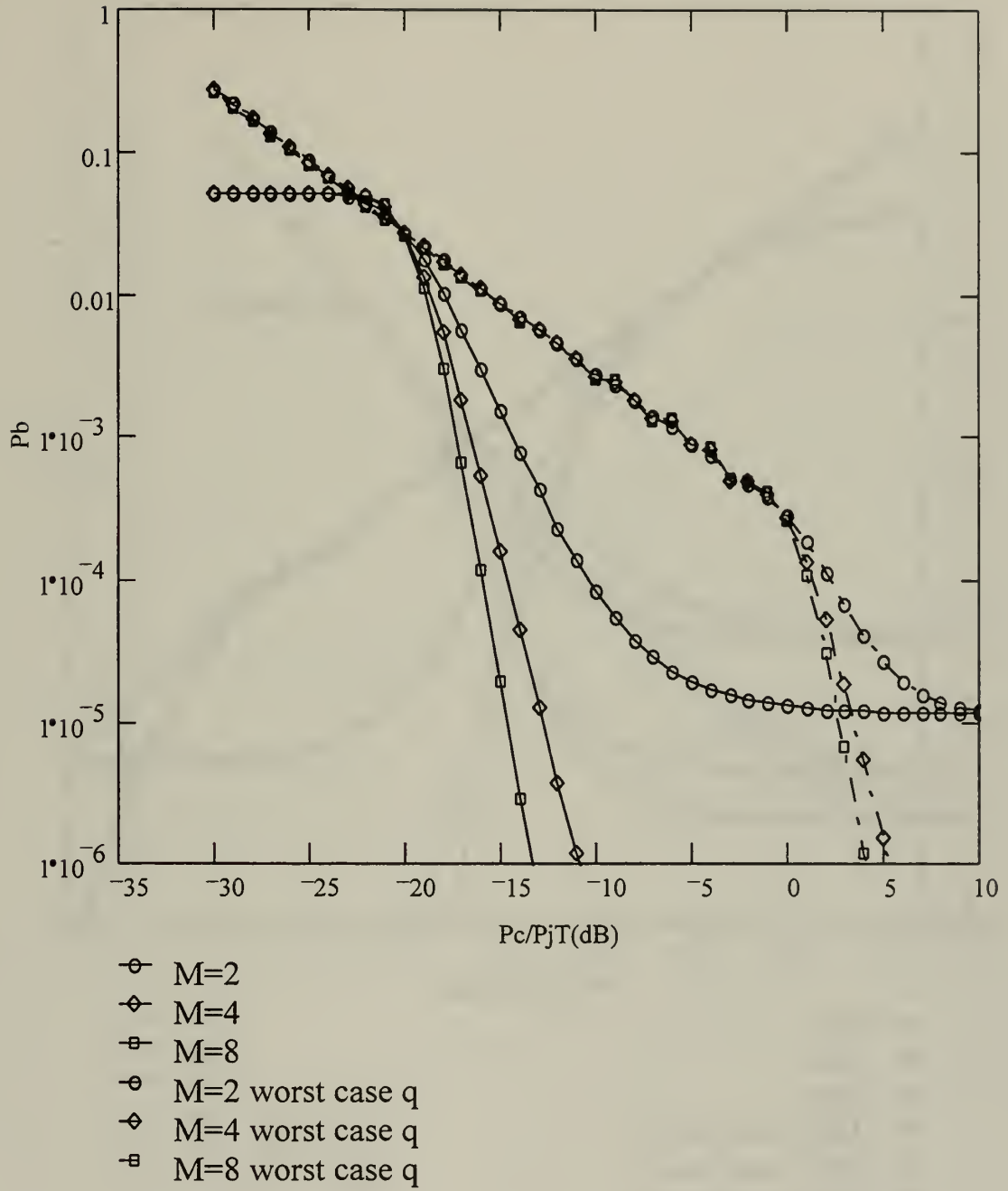


Figure 10: Checking the Union Bound accuracy for essentially no fading of the information signal for band multitone interference with no fading of the jammer tones, for both $q = 100$ and q_{wc} , for $M = 2, 4$, and 8 . No anomaly detected for the P_b using the union bound and P_b decreases as M increases.

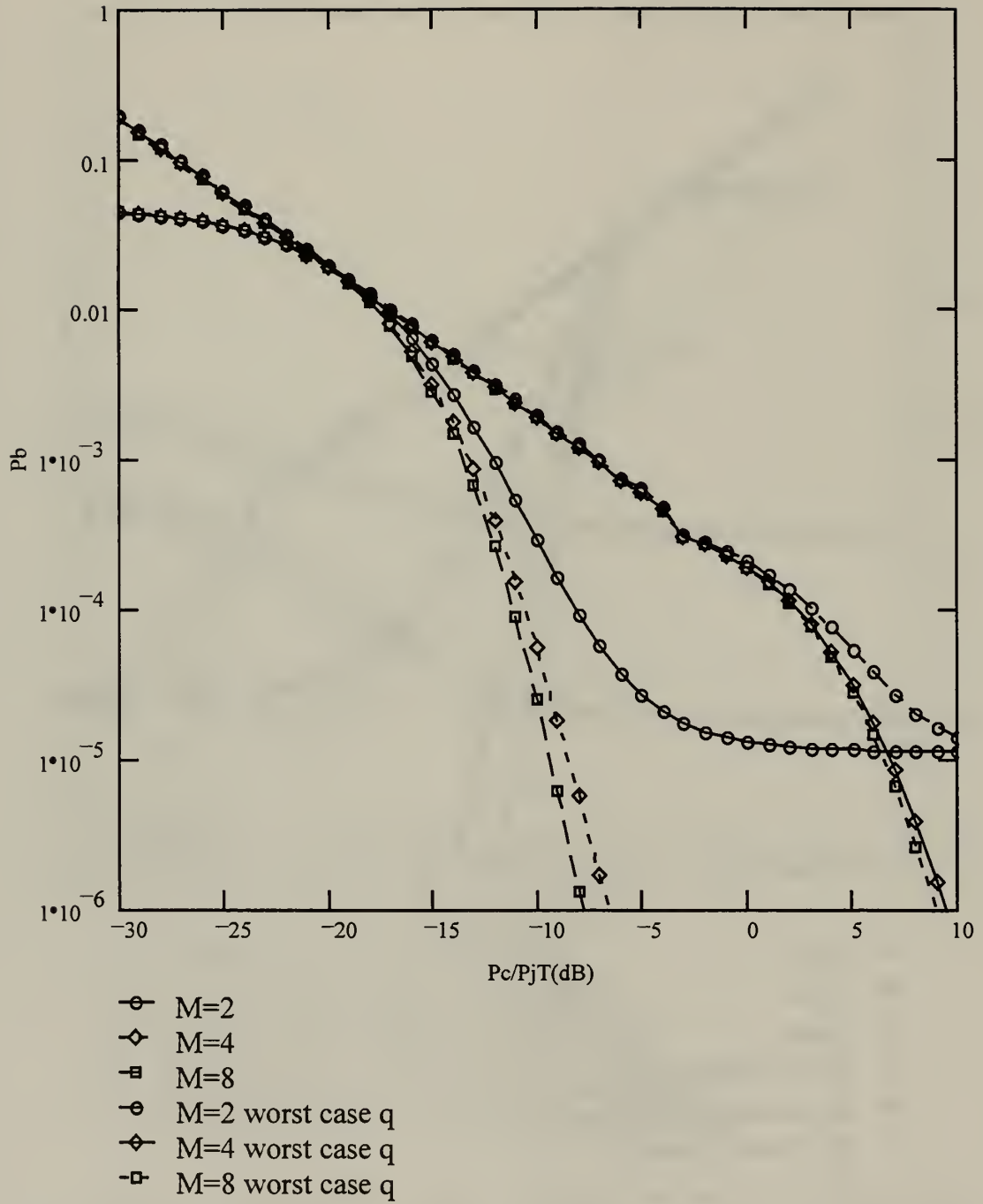


Figure 11: Checking the Union Bound accuracy for essentially no fading of the information signal for band multitone interference with Rayleigh fading of the jammer tones, for both $q = 100$ and q_{wc} , for $M = 2, 4$, and 8. No anomaly detected for the P_b using the union bound and P_b decreases as M increases.

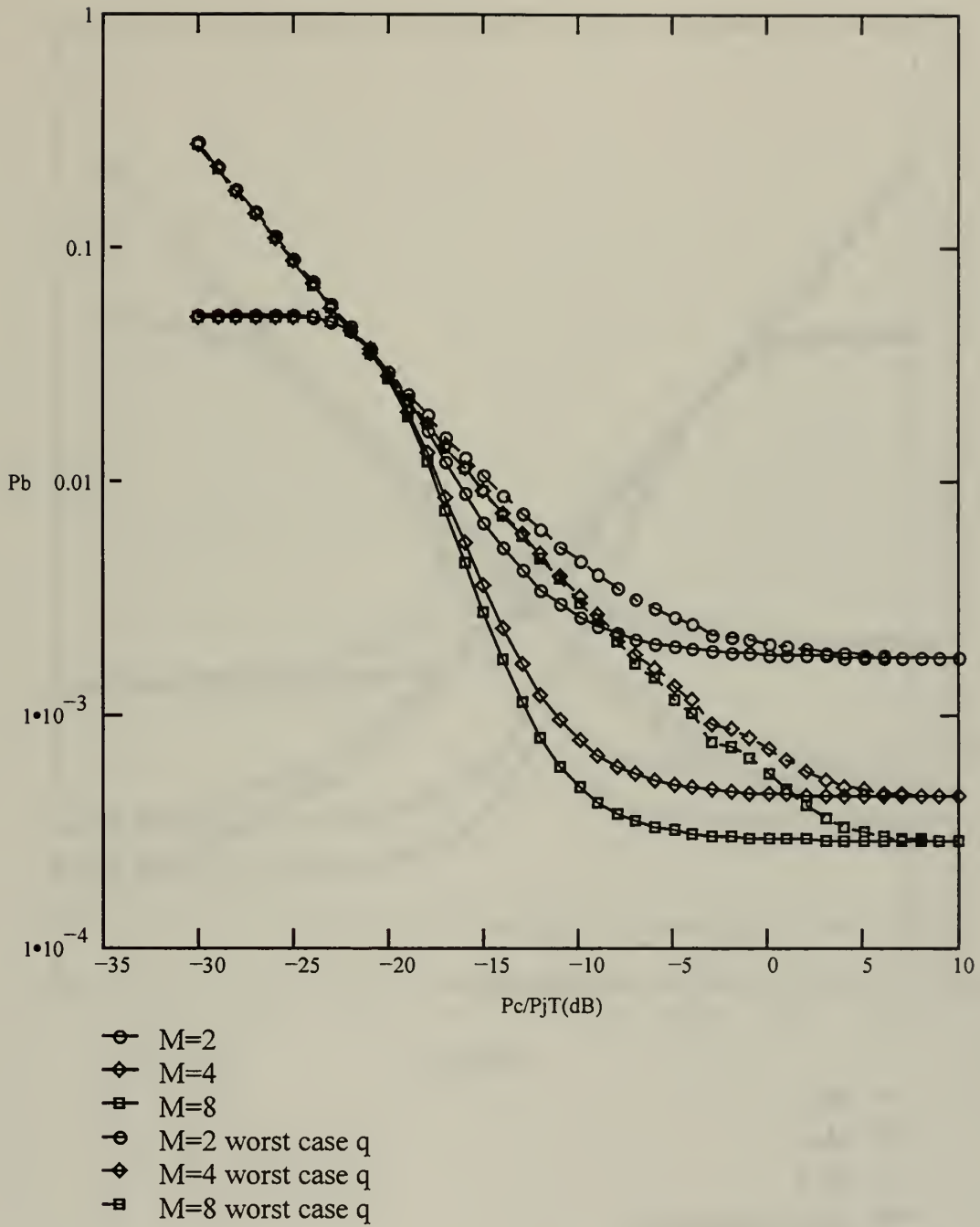


Figure 12: Checking the Union Bound accuracy for Ricean fading of the information signal for band multitone interference with essentially no fading of the jammer tones, for both $q = 100$ and q_{wc} , for $M = 2, 4$, and 8 . No anomaly detected for the P_b using the union bound and P_b decreases as M increases.

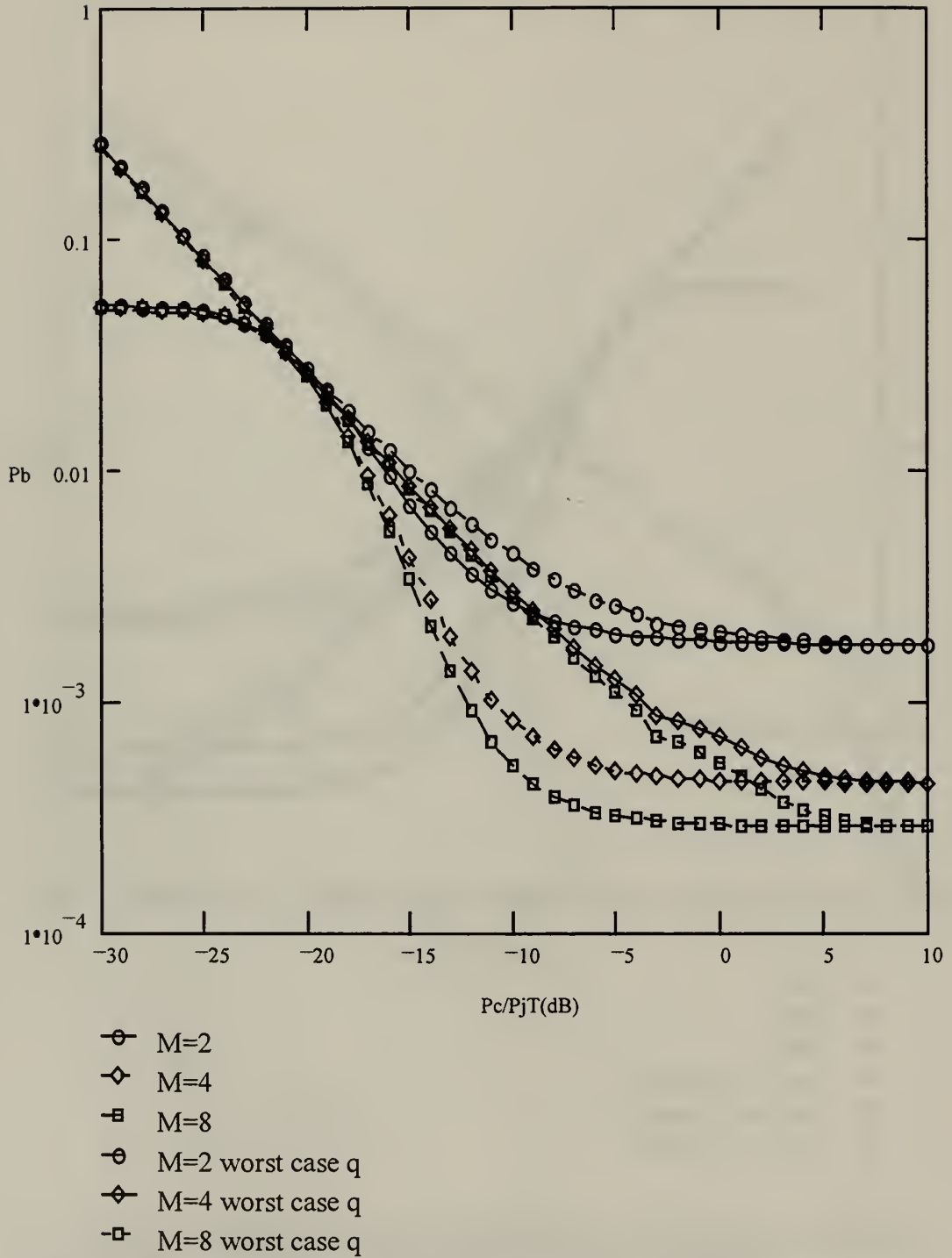


Figure 13: Checking the Union Bound accuracy for Ricean fading of the information signal for band multitone interference with Ricean fading of the jammer tones, for both $q = 100$ and q_{wc} , for $M = 2, 4, \text{ and } 8$. No anomaly detected for the P_b using the union bound and P_b decreases as M increases.

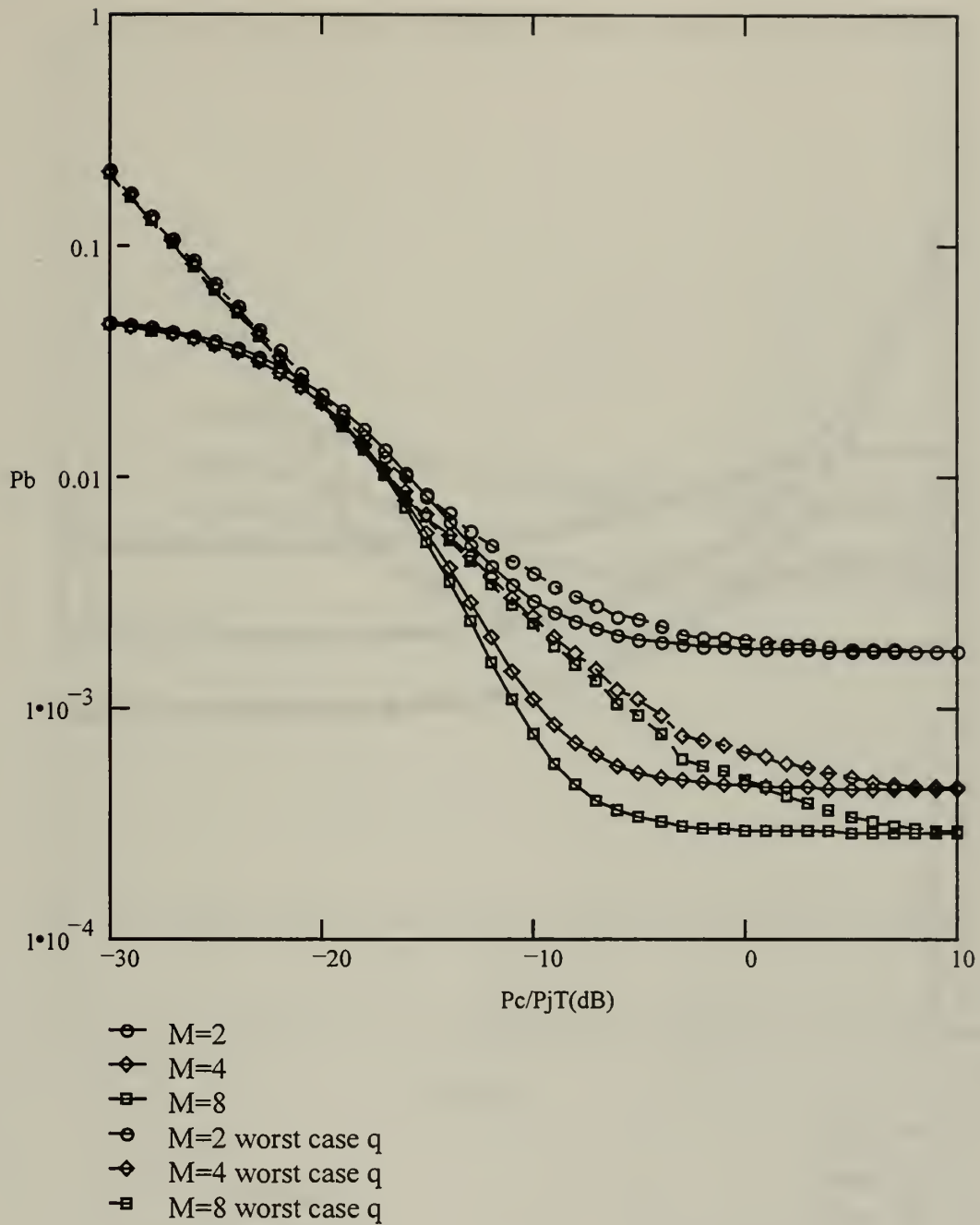
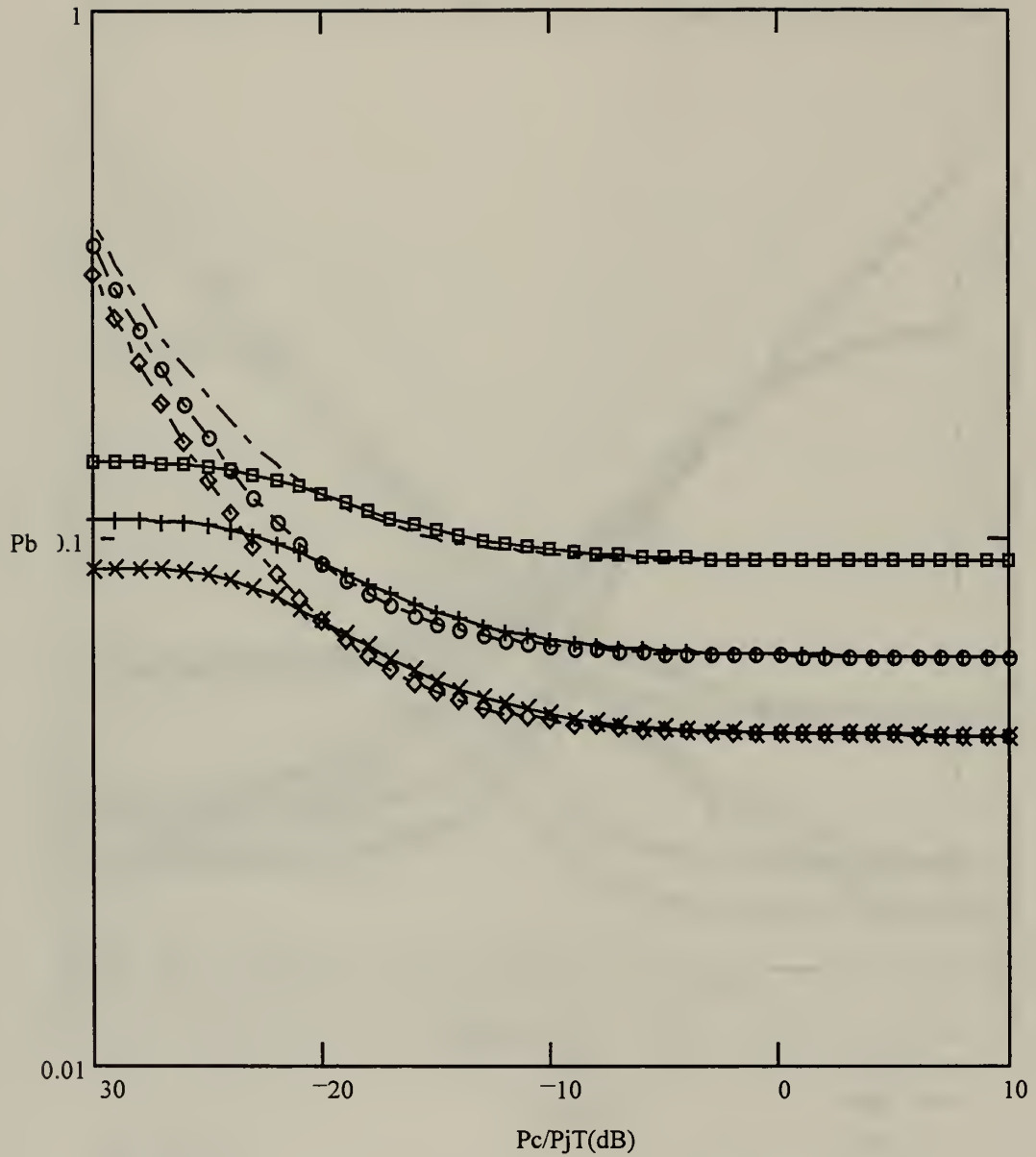


Figure 14: Checking the Union Bound accuracy for Ricean fading of the information signal for band multitone interference with Rayleigh fading of the jammer tones, for both $q = 100$ and q_{wc} , for $M = 2, 4$, and 8 . No anomaly detected for the P_b using the union bound and P_b decreases as M increases.



- × M=2
- + M=8
- ▣ M=16
- ◊ M=2 worst case q
- M=8 worst case q
- M=16 worst case q

Figure 15 : Checking the Union Bound accuracy for Rayleigh fading of the information signal for band multitone interference with essentially no fading of the jammer tones, for both $q = 100$ and q_{wc} , for $M = 2, 8$, and 16 . Anomaly detected!!! For increasing M the probability of error increases.

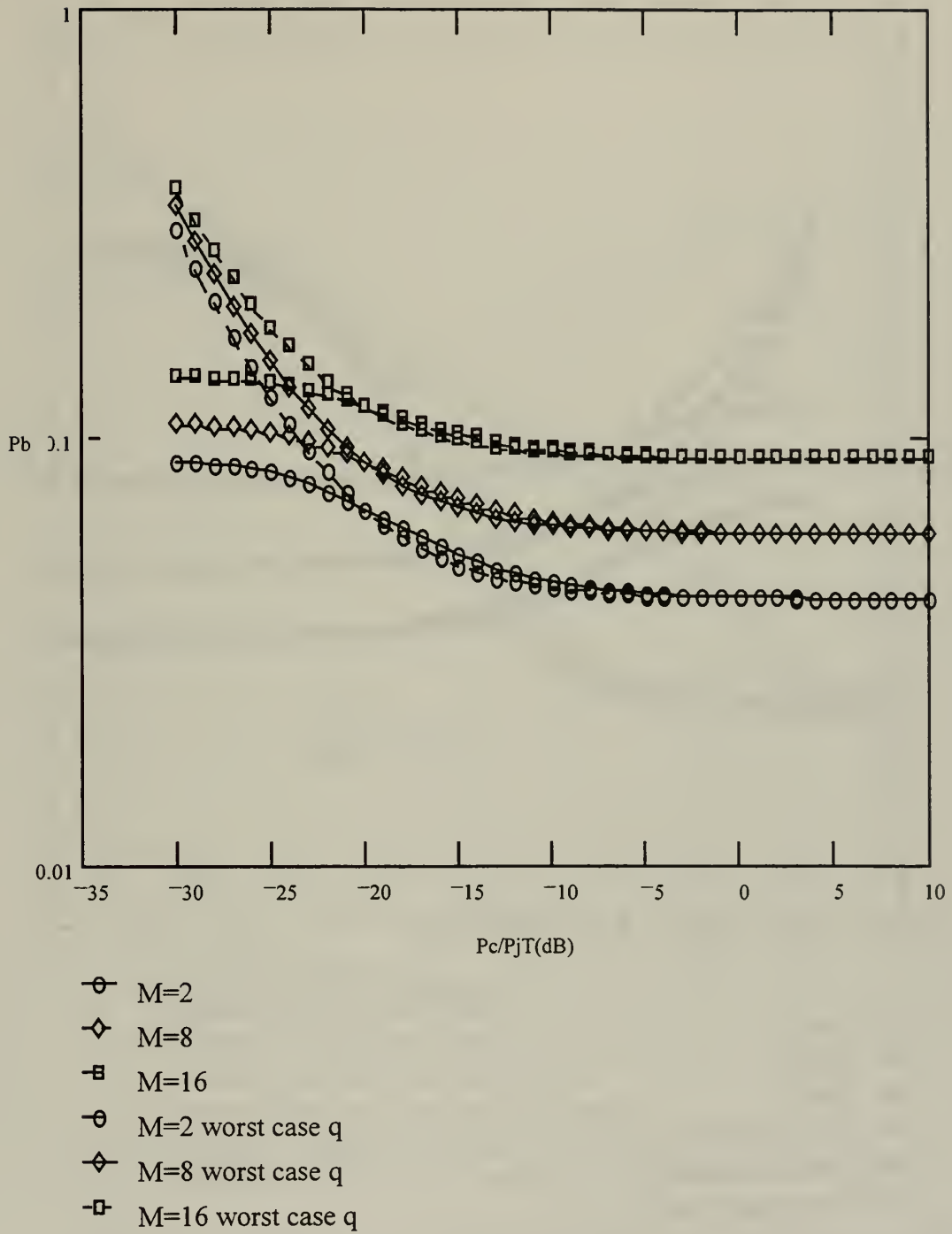


Figure 16 : Checking the Union Bound accuracy for Rayleigh fading of the information signal for band multitone interference with Ricean fading of the jammer tones, for both $q = 100$ and q_{wc} , for $M = 2, 8$, and 16 . Anomaly detected!!! For increasing M the probability of error increases.

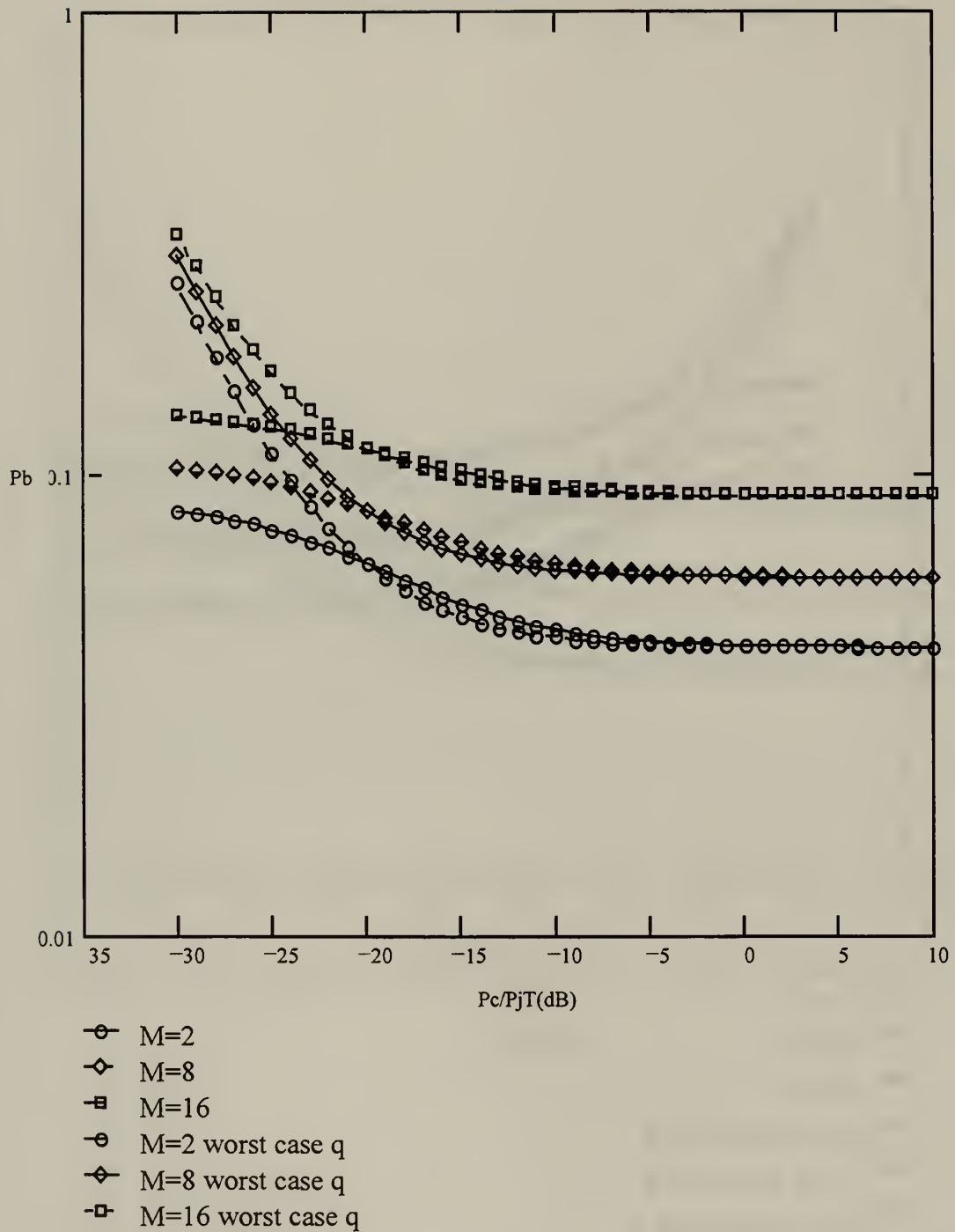
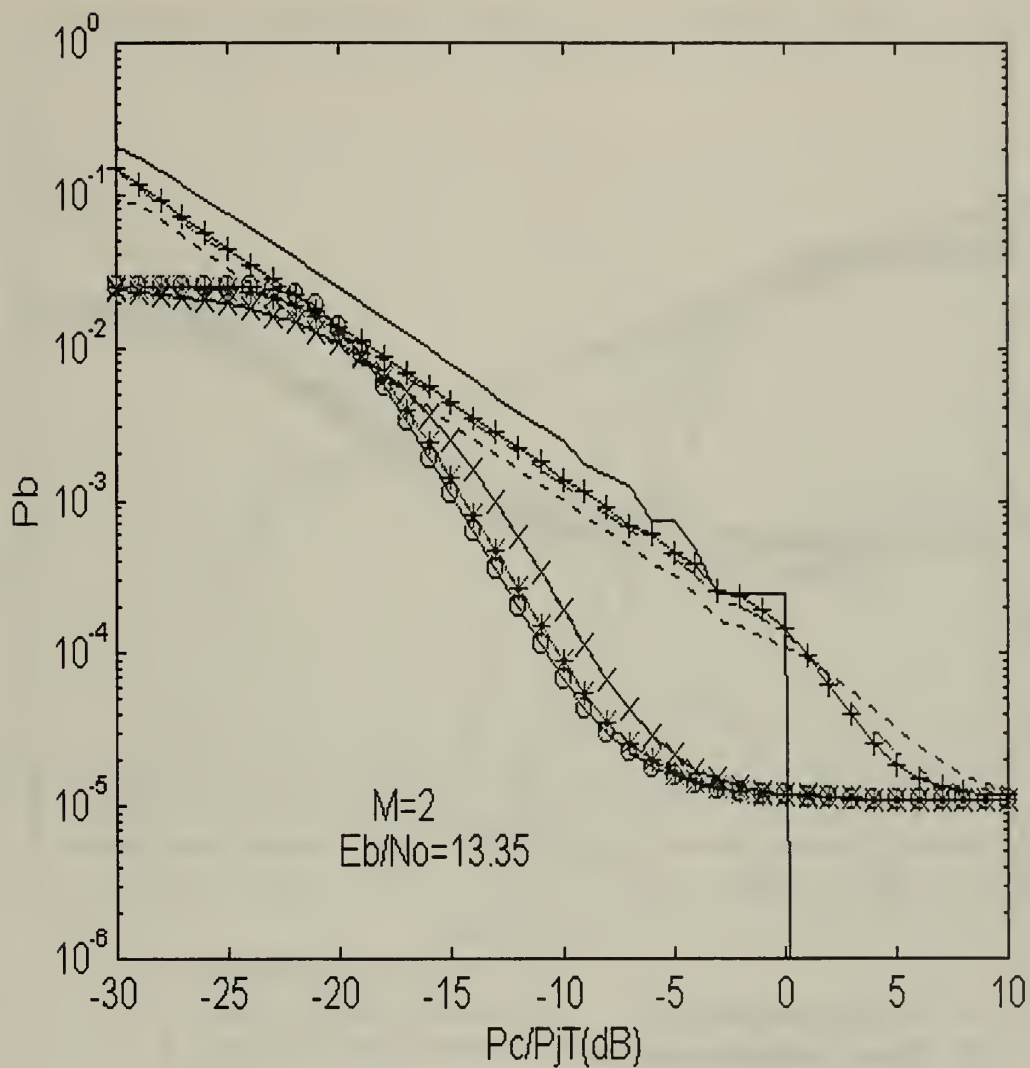
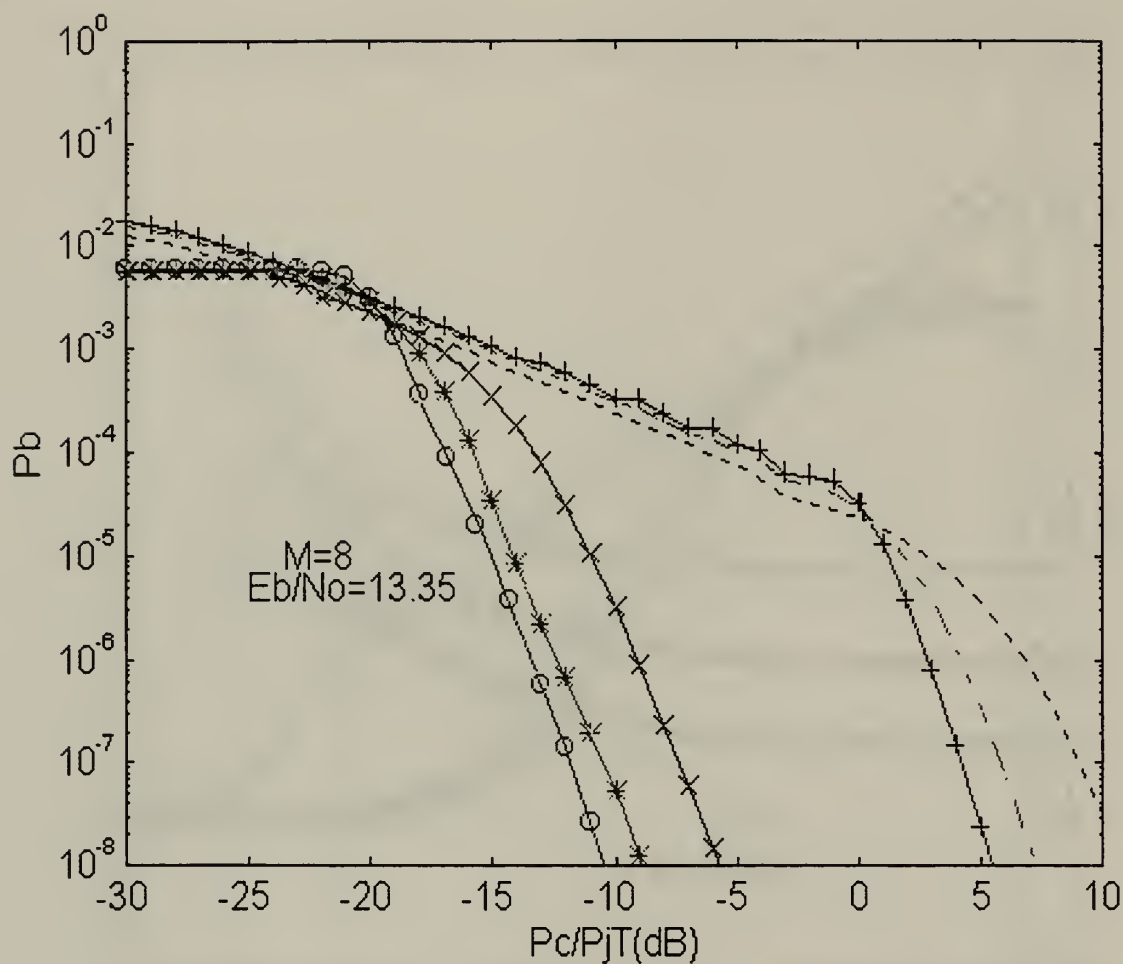


Figure 17: Checking the Union Bound accuracy for Rayleigh fading of the information signal for band multitone interference with Rayleigh fading of the jammer tones, for both $q = 100$ and q_{wc} , for $M = 2, 8, \text{ and } 16$. Anomaly detected!!! For increasing M the probability of error increases.



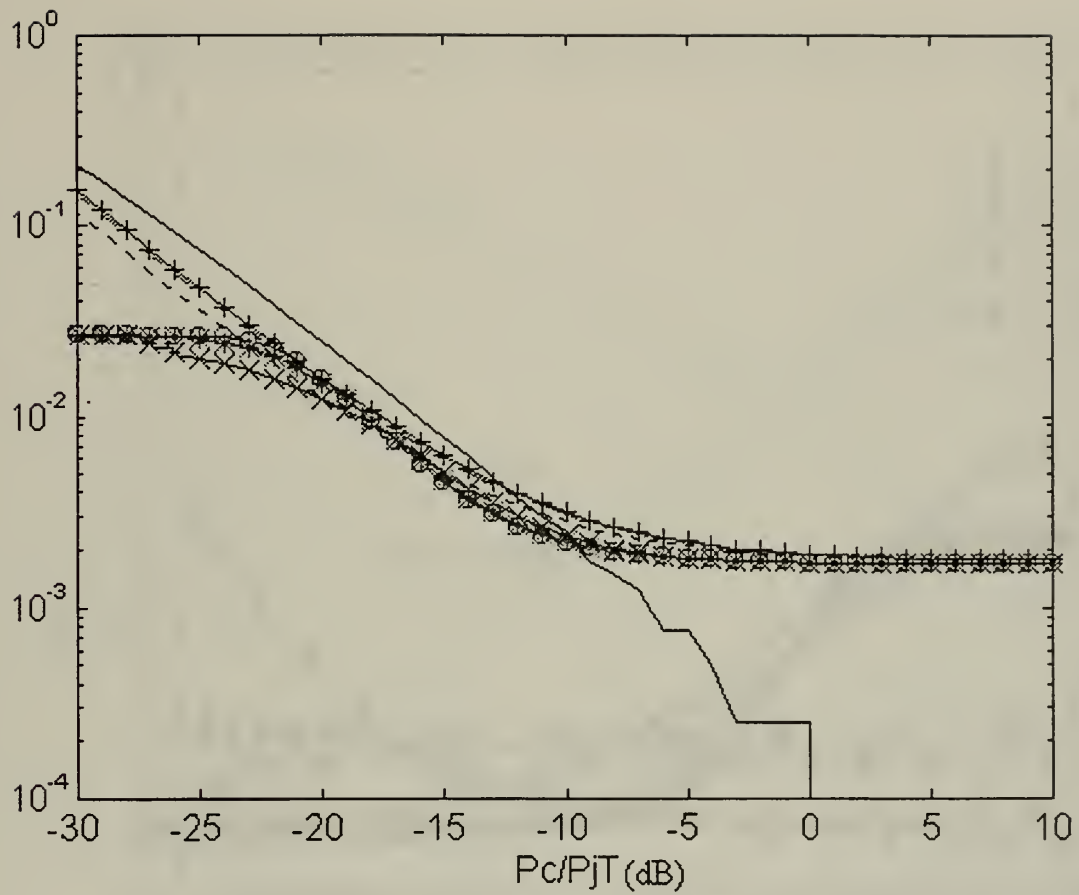
- o No fading jammer tone
- * Ricean Fading jammer tone
- x Rayleigh Fading jammer tone
- + No fading jammer tone worst case q
- Ricean Fading jammer tone worst case q
- - Rayleigh Fading jammer tone worst case q
- ... Performance for zero thermal noise

Figure 18: Performance of a FH/BFSK noncoherent receiver with essentially no information signal fading for independent multitone interference with various conditions of fading of the multiple interference tones. The results are identical with the ones obtained using the exact result equations.



- o No fading jammer tone
- * Ricean Fading jammer tone
- x Rayleigh Fading jammer tone
- + No fading jammer tone worst case q
- Ricean Fading jammer tone worst case q
- - Rayleigh Fading jammer tone worst case q

Figure 19: Performance of a FH/8FSK non-coherent receiver with essentially no signal fading and various interference fading for independent multitone interference.



- o No fading jammer tone
- * Ricean Fading jammer tone
- x Rayleigh Fading jammer tone
- + No fading jammer tone worst case q
- Ricean Fading jammer tone worst case q
- Rayleigh Fading jammer tone worst case q
- ... Performance for zero thermal noise

Figure 20: Performance of a FH/BFSK non-coherent receiver with Ricean signal fading and various interference fading for independent multitone interference.

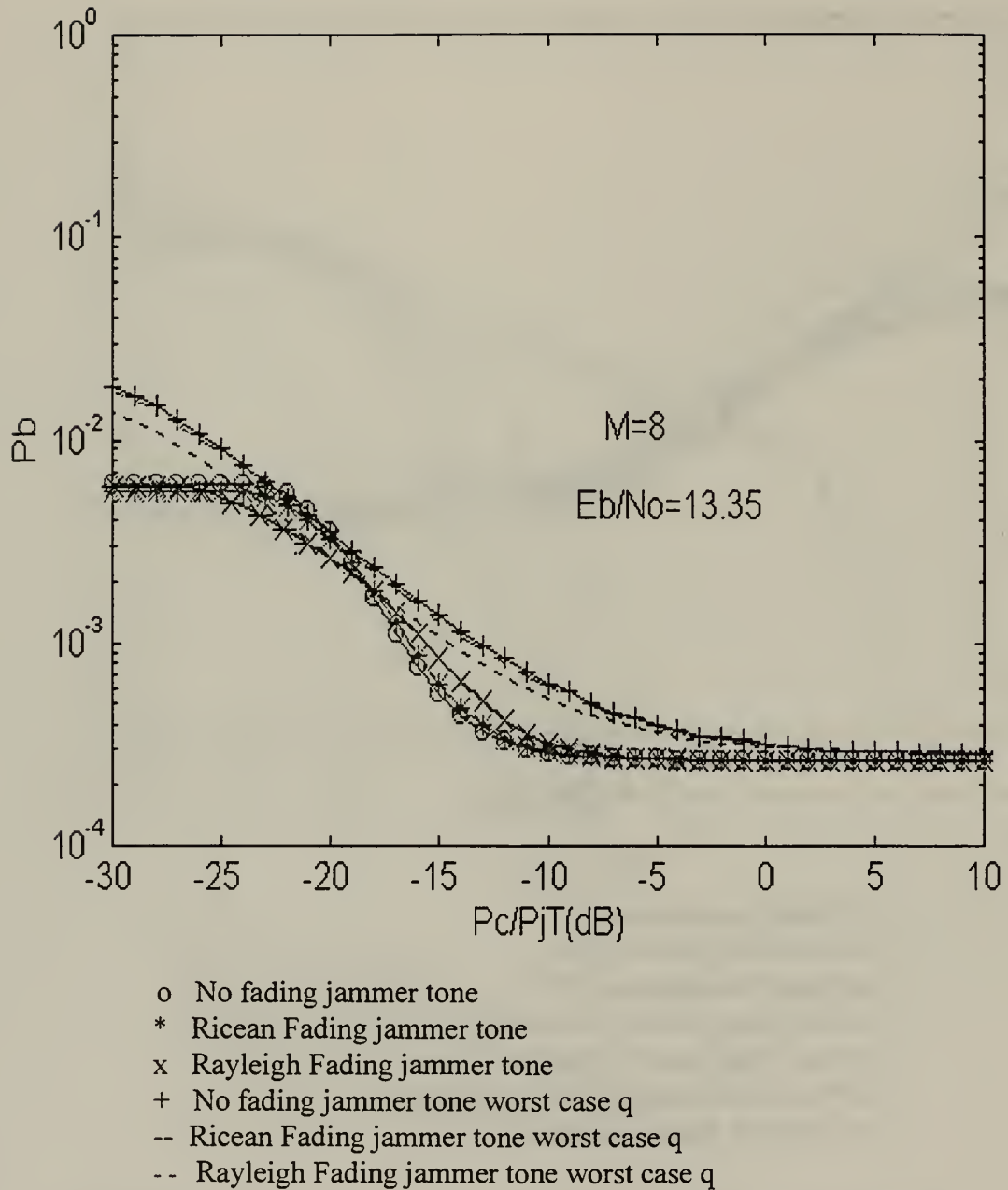


Figure 21: Performance of a FH/8FSK non-coherent receiver with Ricean signal fading and various interference fading for independent multitone interference.

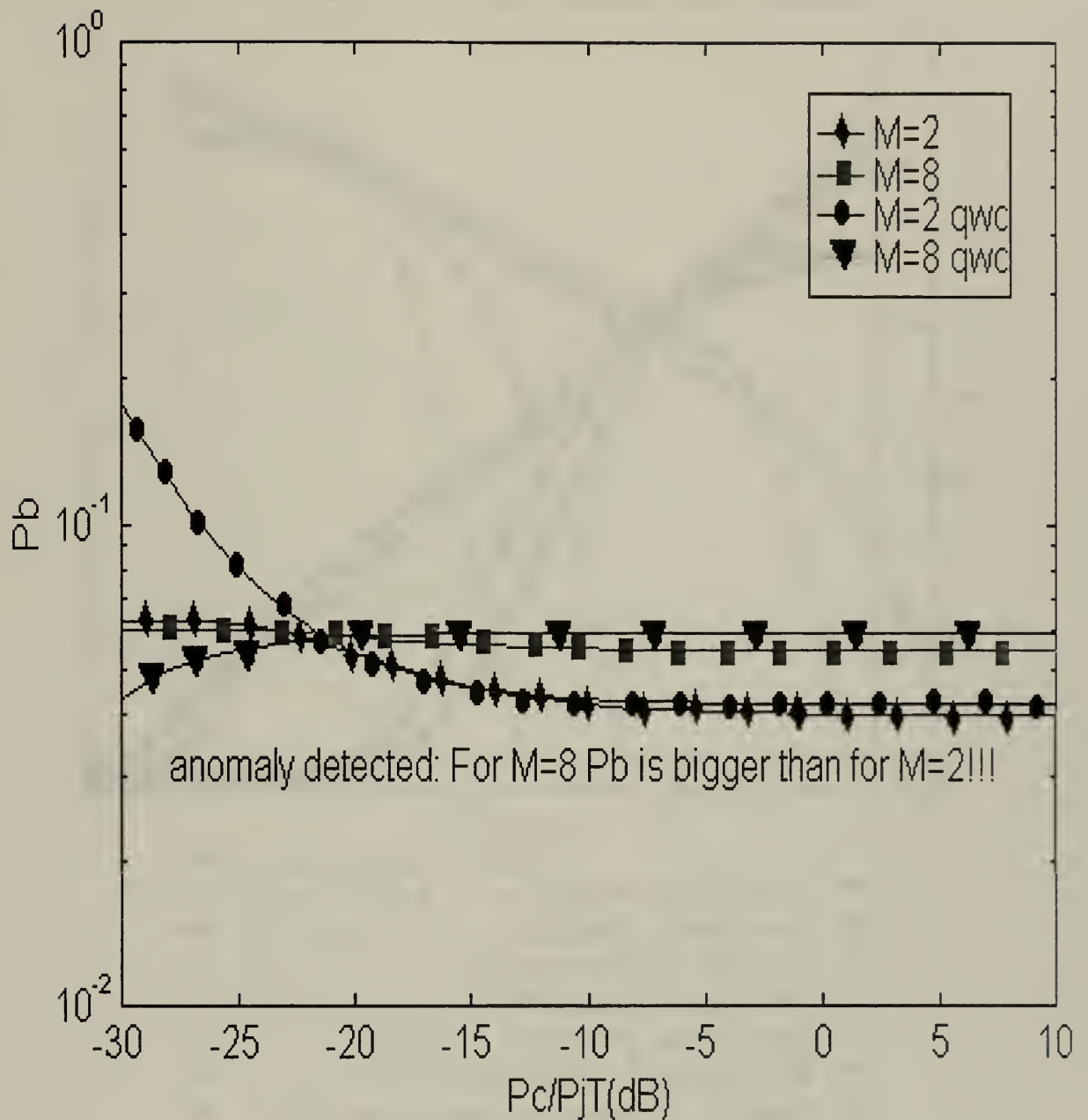


Figure 22: Performance of a FH/BFSK and FH/8FSK receiver for Rayleigh fading information signal and non-fading interference, for independent multitone interference. Anomaly detected, since for an increase in M we notice an increase to the probability of error.

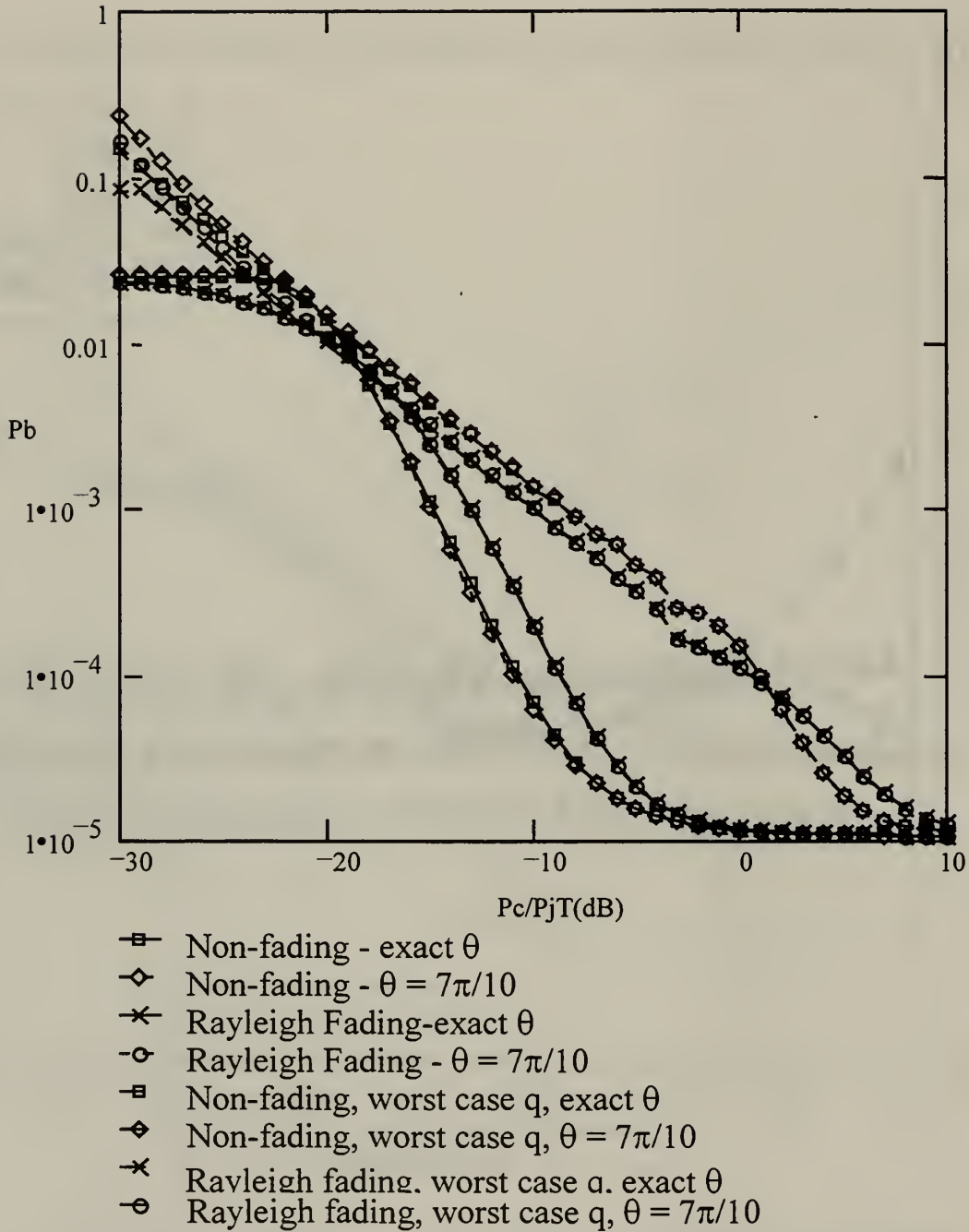


Figure 23: A comparison of the union bound curves for a FH/BFSK noncoherent receiver's performance with essentially no information signal fading for independent multitone interference with either no fading or Rayleigh fading of the jammer tones, with $q = 100$ and worst case q , obtained by integrating θ and also by approximating θ with $\frac{7}{10}\pi$. The results obtained are identical, so the approximation can effectively be used simplifying the calculations.

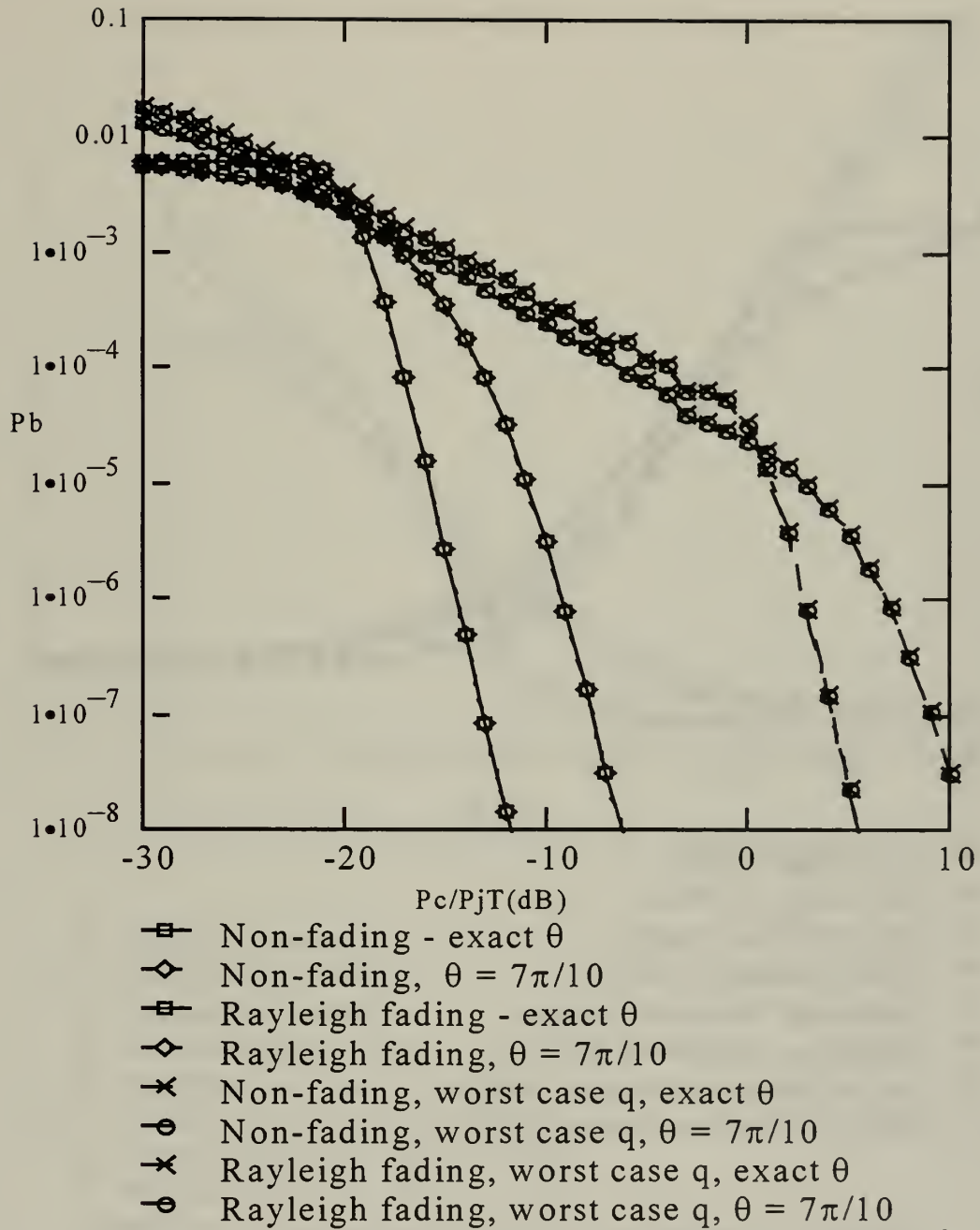


Figure 24: A comparison of the union bound curves for a FH/8FSK noncoherent receiver's performance with essentially no information signal fading for independent multitone interference with either no fading or Rayleigh fading of the jammer tones, with $q = 100$ and worst case q , obtained by integrating θ and also by approximating θ with $\frac{7}{10}\pi$. The results obtained are identical, so the approximation can effectively be used simplifying the calculations.

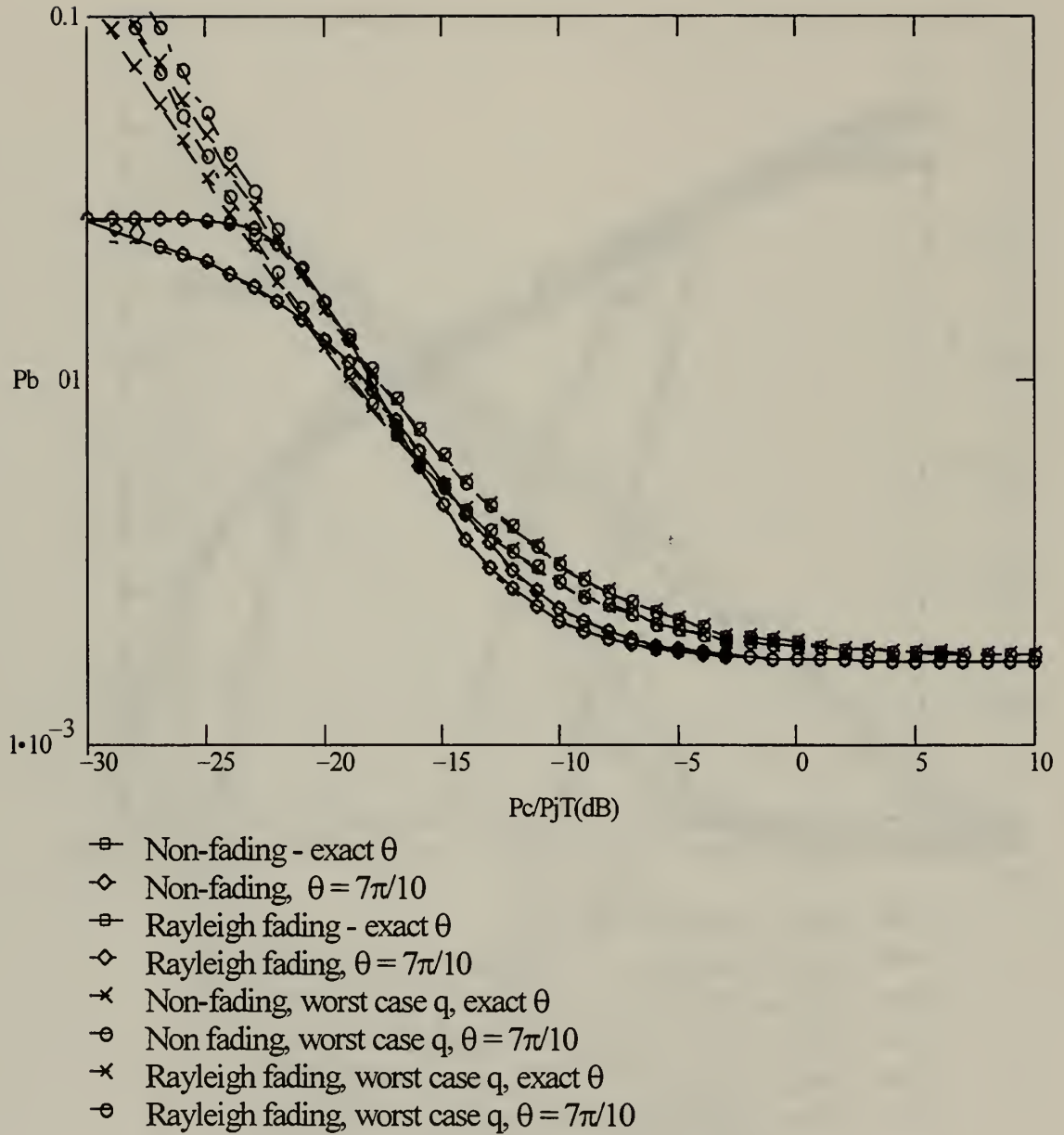


Figure 25: A comparison of the union bound curves for a FH/BFSK noncoherent receiver's performance with Ricean information signal fading for independent multitone interference with either no fading or Rayleigh fading of the jammer tones, with $q = 100$ and worst case q, obtained by integrating θ and also by approximating θ with $\frac{7}{10}\pi$. The results obtained are identical, so the approximation can effectively be used simplifying the calculations.

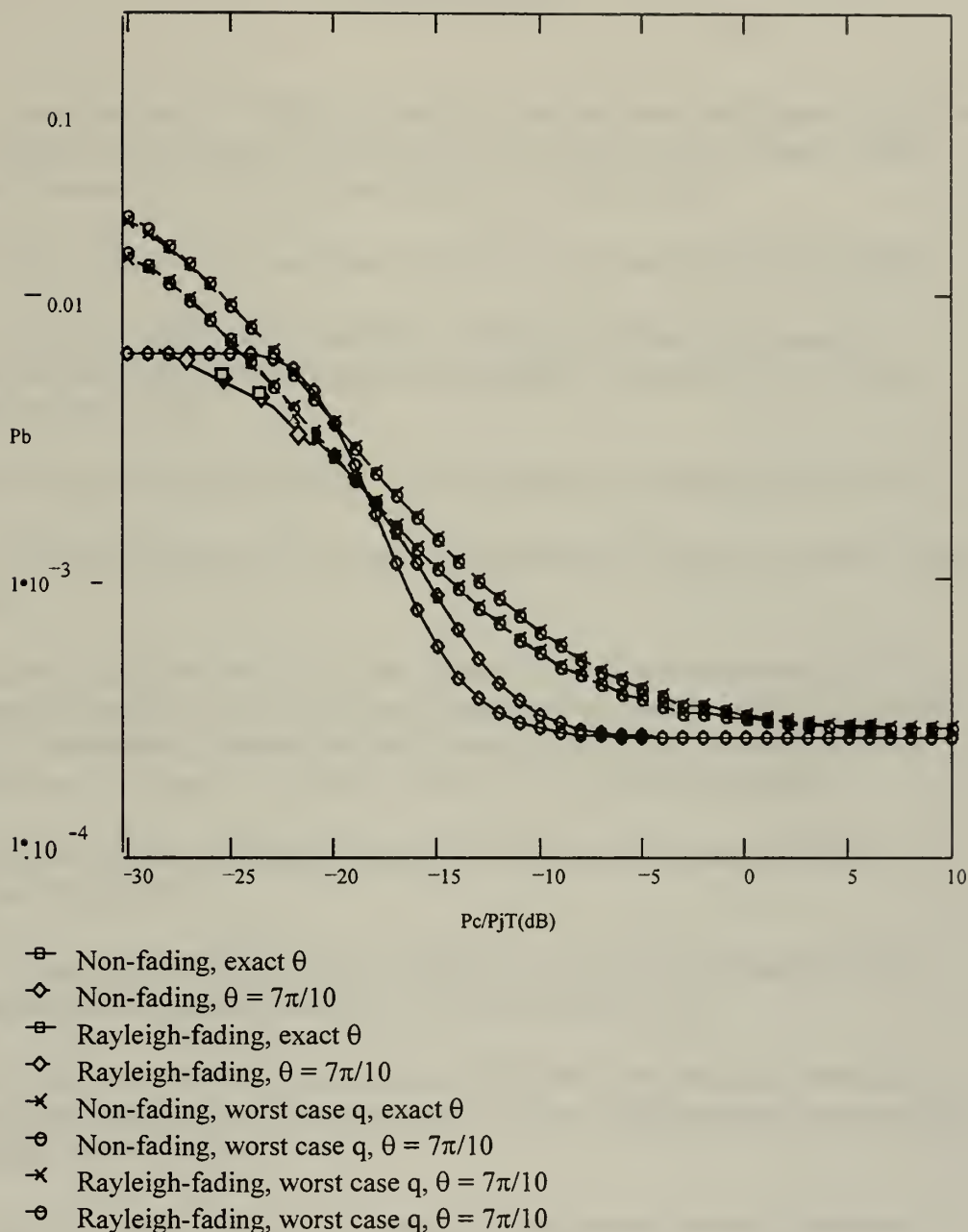


Figure 26: A comparison of the Union Bound Curves for a FH/8FSK noncoherent receiver's performance with Ricean information signal fading for independent multitone interference with either no fading or Rayleigh fading of the jammer tones, with $q = 100$ and worst case q , obtained by integrating θ and also by approximating θ with $\frac{7}{10}\pi$. The results obtained are identical, so the approximation can effectively be used simplifying the calculations.



x	y	x	y
0	0	4	16
1	1	3	9
2	4	2	4
3	9	1	1
4	16	0	0

The graph illustrates the relationship between the function $y = x^2$ and its inverse $y = \sqrt{x}$. The curves are symmetric with respect to the line $y = x$. The intersection points of the two curves are $(0,0)$, $(1,1)$, and $(4,2)$. The domain of $y = x^2$ is $[-\infty, \infty]$ and the range is $[0, \infty)$. The domain of $y = \sqrt{x}$ is $[0, \infty)$ and the range is $[-\infty, \infty]$.

REFERENCES

1. R. C. Robertson and J. F. Sheltry, "Multiple Tone Interference of Frequency-Hopped Noncoherent MFSK Signals Transmitted Over Ricean Fading Channels," *IEEE Trans. Commun.*, vol. COM-44, no. 7, pp. 867-875, Jul. 1996.
2. J. G. Proakis, *Digital Communications*, 2nd Ed., New York: McGraw Hill, 1989.
3. I. S. Gradshteyn and I. M. Ryzhik, *Table of Integrals, Series, and Products*, Corrected and Enlarged Ed., translated and edited by Alan Jeffrey. New York: Academic Press, 1980.
4. A. D. Whalen, *Detection of Signals in Noise*, New York: Academic Press, 1971.
5. H. L. Van Trees, *Detection, Estimation, and Modulation Theory*. New York: Wiley, 1968.
6. J. S. Lee, L. E. Miller, and Y. K. Kim, "Probability of error analysis of a BFSK frequency-hopping system with diversity under partial-band jamming interference Part II: Performance of square-law non linear combining soft decision receivers" *IEEE Trans. Commun.*, vol. COM-32, no. 12, pp. 1243-1250, Dec. 1984.
7. P. M. Morse, Herman Feshback, *Methods of Theoretical Physics*, New York: McGraw Hill, 1953.
8. R. L. Peterson, R. E. Ziemer, and D. E. Borth, *Introduction to Spread Spectrum Communications*, Englewood Cliffs, NJ: Prentice-Hall, 1995.
9. B. K. Levitt, "Use of diversity to improve FH/MFSK performance in worst case partial band noise and multitone jamming," in *Proc. IEEE Military Commun. Conf.*, 1982, pp. 28.2-1 - 28.2-5.
10. J. S. Lee, L. E. Miller, and R. H. French, "The analyses of uncoded performances for certain ECCM receiver design strategies for multihops/symbol FH/MFSK waveforms," *IEEE J. Selected Areas Commun.*, vol. SAC-3, pp. 611-620, Sept. 1985.
11. M. Abramowitz and I. A. Stegun, *Handbook of Mathematical Functions*. New York: Dover Publications, 1972.

12. W. C. Lindsey, "Error probabilities for Rician fading multichannel reception of binary and N-ary signals," *IEEE Trans. on Infor. Theory*, vol. IT-10, pp. 339-350 Oct. 1964.
13. Simon Haykin, *Communication Systems*, 3rd Ed., New York: John Wiley & Sons, Inc. 1994.

APPENDIX . MATHEMATICAL IDENTITIES AND RELATIONS

For convenience, all pertinent equations are repeated here.

A. IDENTITIES

1. Integrals

$$\bullet I_n(z) = \exp\left(-\frac{jn\pi}{2}\right) \cdot J_n(jz) = (-j)^n \cdot J_n(jz) \quad (\text{A.1})$$

$$\bullet I_0(z) = \frac{1}{2\pi} \cdot \int_0^{2\pi} \exp[\pm z \cdot \cos(\phi - \theta)] d\phi \quad (\text{A.2})$$

$$\bullet \int_0^\infty x^{\frac{m+n}{2}} \cdot e^{-ax} \cdot J_n(2\beta\sqrt{x}) dx = \frac{m! \beta^n \exp\left[-\frac{\beta^2}{a}\right]}{a^{m+n+1}} \mathfrak{I}_m^n\left(\frac{\beta^2}{a}\right)$$

where $\mathfrak{I}_m^n(\bullet)$ is the Laguerre polynomial:

$$\mathfrak{I}_m^n\left(\frac{\beta^2}{a}\right) = \sum_{p=0}^m \frac{(-1)^p}{p!} \cdot \binom{m+n}{m-p} \cdot \left(\frac{\beta^2}{a}\right)^p. \quad (\text{A.3})$$

$$\bullet \int_0^\infty x \cdot \exp[-ax^2] \cdot I_n(\beta x) \cdot J_n(\gamma x) dx = \frac{1}{2a} \cdot \exp\left[\frac{\beta^2 - \gamma^2}{4a}\right] \cdot J_n\left(\frac{\beta\gamma}{2a}\right) \quad (\text{A.4})$$

2. The Marcum's Q function and related integrals

$$\bullet Q(a, \beta) = \int_{\beta}^{\infty} x \cdot \exp\left(-\frac{x^2 + a^2}{2}\right) \cdot I_0(ax) dx \quad (A.5)$$

$$\bullet Q(a, 0) = 1 \quad (A.6)$$

$$\bullet Q(0, \beta) = \exp\left(-\frac{\beta^2}{2}\right) \quad (A.7)$$

$$\bullet Q(a, \beta) = 1 - Q(\beta, a) + \exp\left(-\frac{a^2 + \beta^2}{2}\right) \cdot I_0(a, \beta) \quad (A.8)$$

$$\bullet \int_0^{\infty} Q\left(\frac{a_2}{\sigma_2}, \frac{R_1}{\sigma_2}\right) \cdot \frac{R_1}{\sigma_1^2} \cdot \exp\left(-\frac{a_1^2 + R_1^2}{2\sigma_1^2}\right) \cdot I_0\left(\frac{a_1 R_1}{\sigma_1^2}\right) dR_1 =$$

$$\frac{\sigma_1^2}{\sigma_1^2 + \sigma_2^2} \cdot \left[1 - Q\left(\sqrt{\frac{a_1^2}{\sigma_1^2 + \sigma_2^2}}, \sqrt{\frac{a_2^2}{\sigma_1^2 + \sigma_2^2}}\right) \right] + \frac{\sigma_2^2}{\sigma_1^2 + \sigma_2^2} \cdot Q\left(\sqrt{\frac{a_2^2}{\sigma_1^2 + \sigma_2^2}}, \sqrt{\frac{a_1^2}{\sigma_1^2 + \sigma_2^2}}\right) \quad (A.9)$$

B. RELATIONS

1. Union bound on the probability of bit error

$$\begin{aligned} P_s &= \Pr(R_1 < R_2 \cup R_1 < R_3 \cup \dots \cup R_1 < R_M | 1) \\ &\leq \Pr(R_1 < R_2 | 1) + \Pr(R_1 < R_3 | 1) + \dots + \Pr(R_1 < R_M | 1) \\ &\leq (M - 1) \cdot \Pr(R_1 < R_2 | 1) \end{aligned} \quad (B.1)$$

where by R_1, R_2, \dots, R_M we express the random variables representing the outputs of branches 1, 2, ..., M, respectively, of an MFSK receiver.

2. pdf of a signal's or jammer's amplitude modeled as a Ricean random variable

$$f_{A_i}(a_i) = \frac{a_i}{\sigma_i^2} \cdot \exp\left(-\frac{a_i^2 + \alpha_i^2}{2\sigma_i^2}\right) \cdot I_0\left(\frac{a_i^2 \cdot \alpha_i^2}{\sigma_i^2}\right) \cdot u(a_i) \quad (i = c, j) \quad (B.2)$$

where $u(\bullet)$ is the unit step function, $I_0(\bullet)$ is the modified Bessel function of the first kind and order zero, α_i^2 is the power of the direct signal component, and $2\sigma_i^2$ is the power of the diffuse signal component of the respective tone.

3. pdf of a signal's or jammer's amplitude modeled as a Rayleigh random variable

$$f_{A_i}(a_i) = \frac{a_i}{\sigma_i^2} \cdot \exp\left(-\frac{a_i^2}{2\sigma_i^2}\right) \cdot u(a_i) \quad (i = c, j) \quad (B.3)$$

4. Signal-to-noise power ratio of the direct signal components

$$\rho_i = \frac{\alpha_i^2}{\sigma_n^2} \quad (i = c, j) \quad (B.4)$$

5. Signal-to-noise power ratio of the diffuse signal components

$$\xi_i = \frac{2\sigma_i^2}{\sigma_n^2} \quad (i = c, j) \quad (B.5)$$

6. $\Pr(R_1 < R_2 | l)$

$$\Pr(R_1 < R_2 | l) = \frac{1}{2 + \xi_c} \cdot \exp\left[-\frac{\rho_c}{2 + \xi_c}\right] \quad (\text{B.6})$$

7. $\Pr(R_1 < R_2 | l, S_{j_1})$

$$\Pr(R_1 < R_2 | l, S_{j_1}) = \frac{1}{\xi_j + \xi_c + 2} \cdot \exp\left(-\frac{\rho_c + \rho_j}{\xi_j + \xi_c + 2}\right) \cdot I_0\left(\frac{2\sqrt{\rho_c \rho_j}}{\xi_j + \xi_c + 2}\right) \quad (\text{B.7})$$

8. $\Pr(R_1 < R_2 | l, S_{j_2})$

$$\begin{aligned} \Pr(R_1 < R_2 | l, S_{j_2}) = & Q\left(\frac{\sqrt{2\rho_j}}{\sqrt{2 + \xi_c + \xi_j}}, \frac{\sqrt{2\rho_c}}{\sqrt{2 + \xi_c + \xi_j}}\right) \\ & - \frac{1 + \xi_c}{2 + \xi_c + \xi_j} \cdot \exp\left(-\frac{\rho_c + \rho_j}{2 + \xi_c + \xi_j}\right) \cdot I_0\left(\frac{2\sqrt{\rho_c \rho_j}}{2 + \xi_c + \xi_j}\right) \end{aligned} \quad (\text{B.8})$$

9. $\Pr(R_1 < R_2 | l, S_{j_1}, S_{j_2}, a_c, a_j, \theta)$

$$\begin{aligned} \Pr(R_1 < R_2 | l, S_{j_1}, S_{j_2}, a_c, a_j, \theta) = & \\ & Q\left(\sqrt{\frac{a_j^2}{\sigma_n^2}}, \sqrt{\frac{a_c^2 + a_j^2 + 2a_c a_j \cos(\theta)}{\sigma_n^2}}\right) - \frac{1}{2} \exp\left(-\frac{a_c^2 + 2a_j^2 + 2a_c a_j \cos(\theta)}{2\sigma_n^2}\right) \cdot \\ & I_0\left(\frac{a_j}{\sigma_n} \cdot \sqrt{\frac{a_c^2 + a_j^2 + 2a_c a_j \cos(\theta)}{\sigma_n^2}}\right) \end{aligned} \quad (\text{B.9})$$

$$10. \Pr(R_1 < R_2 | l, S_{j_1}, S_{j_2})$$

$$\Pr(R_1 < R_2 | l, S_{j_1}, S_{j_2}) = \frac{1}{2\pi} \int_0^{2\pi} \int_0^\infty \int_0^\infty \left[Q \left(\sqrt{\frac{a_j^2}{\sigma_n^2}}, \sqrt{\frac{a_c^2 + a_j^2 + 2a_c a_j \cos(\theta)}{\sigma_n^2}} \right) - \frac{1}{2} \right] \cdot \exp \left(\frac{a_c^2 + 2a_j^2 + 2a_c a_j \cos(\theta)}{\sigma_n^2} \right) \cdot I_0 \left(\frac{a_j}{\sigma_n} \cdot \sqrt{\frac{a_c^2 + a_j^2 + 2a_c a_j \cos(\theta)}{\sigma_n^2}} \right) \cdot f_{A_c}(a_c) \cdot f_{A_j}(a_j) da_c da_j d\theta \quad (B.10)$$

11. Probability of symbol error for L jamming tones per hop bin, $1 \leq L \leq M$

$$P_s(L) \leq \frac{L}{M} \cdot \left[(L-1) \cdot \Pr(R_1 < R_2 | l, S_{j_1}, S_{j_2}) + (M-L) \cdot \Pr(R_1 < R_M | l, S_{j_1}) \right] + \left(1 - \frac{L}{M} \right) \cdot \left[L \cdot \Pr(R_1 < R_2 | l, S_{j_2}) + (M-L-1) \cdot \Pr(R_1 < R_M | l) \right] \quad (B.11)$$

12. Probability of symbol error for independent multitone interference for L jamming tones per hop bin, $0 \leq L \leq M$.

$$P_s = \left\{ \prod_{i=0}^{M-1} \left(1 - \frac{q}{N \cdot M - i} \right) \right\} \cdot (M-1) \Pr(R_1 < R_2 | l) + \left\{ \sum_{L=1}^{\min(M-1, q)} \left[\prod_{i=0}^{L-1} \frac{q-i}{M \cdot N - i} \right] \cdot \left[\prod_{i=L}^{M-1} \left(1 - \frac{q-(L-1)-1}{M \cdot N - i} \right) \right] \right\} \cdot P_s(L) + \left\{ \prod_{i=0}^{L-1} \frac{q-i}{M \cdot N - i} \right\} \cdot P_s(M)$$

where the probability $P_s(M)$ is obtained by letting $L=M$ in $P_s(L)$. This yields $P_s(M) = (M-1) \cdot \Pr(R_1 < R_2 | l, S_{j_1}, S_{j_2})$.

So

$$\begin{aligned}
P_s = & \left\{ \prod_{i=0}^{M-1} \left(1 - \frac{q}{N \cdot M - i} \right) \right\} \cdot (M-1) \cdot \frac{1}{2 + \xi_c} \cdot \exp \left(-\frac{\rho_c}{2 + \xi_c} \right) \\
& + \left\{ \sum_{L=1}^{\min(M-1, q)} \left[\prod_{i=0}^{L-1} \frac{q-i}{M \cdot N - i} \right] \cdot \left[\prod_{i=L}^{M-1} \left(1 - \frac{q-(L-1)-1}{M \cdot N - i} \right) \right] \right\} \cdot \frac{L}{M} \\
& \cdot \left[(L-1) \cdot \frac{1}{2\pi} \int_0^{2\pi} \int_0^\infty \int_0^\infty \frac{1}{2} \exp \left(\frac{a_c^2 + a_j^2 + 2a_c a_j \cos(\theta)}{\sigma_n^2} \right) \cdot \right. \\
& \quad \left. \left[Q \left(\sqrt{\frac{a_j^2}{\sigma_n^2}}, \sqrt{\frac{a_c^2 + a_j^2 + 2a_c a_j \cos(\theta)}{\sigma_n^2}} \right) - \right. \right. \\
& \quad \left. \left. I_0 \left(\frac{a_j}{\sigma_n} \cdot \sqrt{\frac{a_c^2 + a_j^2 + 2a_c a_j \cos(\theta)}{\sigma_n^2}} \right) \right] \cdot f_{A_c}(a_c) \cdot f_{A_j}(a_j) da_c da_j d\theta \right. \\
& \quad \left. + (M-L) \cdot \left(\frac{1}{\xi_j + \xi_c + 2} \cdot \exp \left(-\frac{\rho_c + \rho_j}{\xi_j + \xi_c + 2} \right) \cdot I_0 \left(\frac{2\sqrt{\rho_c \rho_j}}{\xi_j + \xi_c + 2} \right) \right) \right] \\
& + \left(1 - \frac{L}{M} \right) \cdot \left[L \left(Q \left(\frac{\sqrt{2\rho_j}}{\sqrt{2 + \xi_c + \xi_j}}, \frac{\sqrt{2\rho_c}}{\sqrt{2 + \xi_c + \xi_j}} \right) - \frac{1 + \xi_c}{2 + \xi_c + \xi_j} \cdot \exp \left(-\frac{\rho_c + \rho_j}{2 + \xi_c + \xi_j} \right) \cdot I_0 \left(\frac{2\sqrt{\rho_c \rho_j}}{2 + \xi_c + \xi_j} \right) \right) \right. \\
& \quad \left. + (M-L-1) \cdot \left(\frac{1}{2 + \xi_c} \cdot \exp \left(-\frac{\rho_c}{2 + \xi_c} \right) \right) \right] \\
& + \left\{ \prod_{i=0}^{L-1} \frac{q-i}{M \cdot N - i} \right\} \cdot (M-1) \cdot \\
& \cdot \left(\frac{1}{2\pi} \int_0^{2\pi} \int_0^\infty \int_0^\infty \frac{1}{2} \exp \left(\frac{a_c^2 + a_j^2 + 2a_c a_j \cos(\theta)}{\sigma_n^2} \right) \cdot \right. \\
& \quad \left[Q \left(\sqrt{\frac{a_j^2}{\sigma_n^2}}, \sqrt{\frac{a_c^2 + a_j^2 + 2a_c a_j \cos(\theta)}{\sigma_n^2}} \right) - \right. \\
& \quad \left. I_0 \left(\frac{a_j}{\sigma_n} \cdot \sqrt{\frac{a_c^2 + a_j^2 + 2a_c a_j \cos(\theta)}{\sigma_n^2}} \right) \right] \cdot f_{A_c}(a_c) \cdot f_{A_j}(a_j) da_c da_j d\theta \left. \right)
\end{aligned} \tag{B.12}$$

13. Probability of symbol error for band multitone interference for L jamming tones per hop bin, $L \geq 1$

$$P_s(L) \leq \frac{q}{N \cdot L} \cdot \left\{ \frac{L}{M} \cdot \left[(L-1) \cdot \Pr(R_1 < R_2 | l, S_{j_1}, S_{j_2}) + (M-L) \cdot \Pr(R_1 < R_2 | l, S_{j_1}) \right] + \right. \\ \left. \left(1 - \frac{L}{M} \right) \cdot \left[L \cdot \Pr(R_1 < R_2 | l, S_{j_2}) + (M-L-1) \cdot \Pr(R_1 < R_2 | l) \right] \right\} + \\ \left(1 - \frac{q}{N \cdot L} \right) \cdot \left((M-1) \frac{1}{2 + \xi_c} \cdot \exp\left(-\frac{\rho_c}{2 + \xi_c}\right) \right)$$

So

$$P_s(L \geq 1) \leq \frac{q}{N \cdot M} \cdot \left[(L-1) \cdot \left[\frac{1}{2\pi} \int_0^{2\pi} \int_0^\infty \int_0^\infty \frac{1}{2} \exp\left(\frac{a^2_c + a^2_j + 2a_c a_j \cos(\theta)}{\sigma^2_n}\right) \cdot \right. \right. \\ \left. \left[Q\left(\sqrt{\frac{a^2_j}{\sigma^2_n}}, \sqrt{\frac{a^2_c + a^2_j + 2a_c a_j \cos(\theta)}{\sigma^2_n}}\right) - \frac{1 + \xi_c}{2 + \xi_c + \xi_j} \right] \cdot \right. \\ \left. \left. I_0\left(\frac{a_j}{\sigma_n} \cdot \sqrt{\frac{a^2_c + a^2_j + 2a_c a_j \cos(\theta)}{\sigma^2_n}}\right) \cdot f_{A_c}(a_c) \cdot f_{A_j}(a_j) da_c da_j d\theta \right] + \right. \\ \left. + (M-L) \cdot \left(\frac{1}{\xi_j + \xi_c + 2} \cdot \exp\left(-\frac{\rho_c + \rho_j}{\xi_j + \xi_c + 2}\right) \cdot I_0\left(\frac{2\sqrt{\rho_c \rho_j}}{\xi_j + \xi_c + 2}\right) \right) \right] \\ + \frac{q}{N \cdot L} \left(1 - \frac{L}{M} \right) \cdot \left[L \left[Q\left(\frac{\sqrt{2\rho_j}}{\sqrt{2 + \xi_c + \xi_j}}, \frac{\sqrt{2\rho_c}}{\sqrt{2 + \xi_c + \xi_j}}\right) - \frac{1 + \xi_c}{2 + \xi_c + \xi_j} \right] \cdot \right. \\ \left. \exp\left(-\frac{\rho_c + \rho_j}{2 + \xi_c + \xi_j}\right) \cdot I_0\left(\frac{2\sqrt{\rho_c \rho_j}}{2 + \xi_c + \xi_j}\right) \right. \\ \left. + (M-L-1) \cdot \left(\frac{1}{2 + \xi_c} \cdot \exp\left(-\frac{\rho_c}{2 + \xi_c}\right) \right) \right] + \\ + \left(1 - \frac{q}{N \cdot L} \right) \cdot \left((M-1) \frac{1}{2 + \xi_c} \cdot \exp\left(-\frac{\rho_c}{2 + \xi_c}\right) \right) \quad (B.13)$$

14. Relation between probability of bit error and probability of symbol error

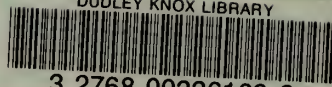
$$P_b = \frac{M/2}{M-1} \cdot P_s, \text{ where } M \text{ is the number of symbols} \quad (\text{B.14})$$

INITIAL DISTRIBUTION LIST

1. Defense Technical Information Center.....2
8725 John J. Kingman Rd., Ste 0944
FT. Belvoir, VA 22060-6218
2. Dudley Knox Library.....2
Naval Postgraduate School
411 Dyer Rd.
Monterey, CA 93943-5101
3. Chairman, Code EC.....1
Department of Electrical and Computer Engineering
Naval Postgraduate School
Monterey, CA 93943-5121
4. Prof. R. Clark Robertson, Code EC/Rc.....2
Department of Electrical and Computer Engineering
Naval Postgraduate School
Monterey, CA 93943-5121
5. Prof. Tri. T. Ha, Code EC/Ha.....1
Department of Electrical and Computer Engineering
Naval Postgraduate School
Monterey, CA 93943-5121
6. Prof. Roberto Cristi, Code EC/Cx.....1
Department of Electrical and Computer Engineering
Naval Postgraduate School
Monterey, CA 93943-5121
7. Prof. Ralph Hippenstiel, Code EC/Hi.....1
Department of Electrical and Computer Engineering
Naval Postgraduate School
Monterey, CA 93943-5121
8. Embassy of Greece.....1
Naval Attache
2228 Massachusetts Ave., N.W.
Washington, DC 20008
9. Lt. JG. George Katsoulis.....3
13 Plaitou St.
Kallipolis, Pireas, 18539
GREECE

DUDLEY KNOX LIBRARY
NAVAL POSTGRADUATE SCHOOL
MONTEREY CA 93943-5101

DUDLEY KNOX LIBRARY



3 2768 00336169 2